Melt-Functionalization of Cellulose Nanocrystals using Dynamic Hindered Ureas

Zehra Oluz†, Nicholas Macke†, Sarah Candelaria, Abrianna Ambus, Aurora Zemborain, Chinwe S. Udemgba, Adam M. Weiss, Céline Calvino, Stuart J. Rowan**

Dr. Z. Oluz[1], N. Macke[1], S. Candelaria[2], A. Ambus[1], A. Zemborain[1], C. S. Udemgba[1], Dr. A. M. Weiss[2], Dr. C. Calvino[1], Prof. S. J. Rowan[1,2,3]

1 Pritzker School of Molecular Engineering, University of Chicago
5640 S. Ellis Ave., Chicago, IL 60637, USA

2 Department of Chemistry, University of Chicago
5735 S Ellis Ave., Chicago, IL 60637, United States

3 Chemical and Engineering Sciences, Argonne National Laboratory
9700 Cass Avenue, Lemont, Illinois 60439, United States

† - denotes equal contribution

Email: stuartrowan@uchicago.edu

Keywords: cellulose nanocrystals, polymer grafting, hindered ureas, melt functionalization, dynamic covalent chemistry

Abstract: Cellulose nanocrystal (CNC)-reinforced composites are gaining commercial attention on account of their high strength and sustainable sourcing. Grafting polymers to the CNCs in these composites has the potential to improve their properties, but current solution-based synthesis methods limit their production at scale. Utilizing dynamic hindered urea chemistry, a new method for the melt-functionalization of cellulose nanocrystals has been developed. This method does not require toxic solvents during the grafting step and can achieve grafting densities competitive with state-of-the-art solution-based grafting methods. Using cotton-sourced, TEMPO-oxidized CNCs, multiple molecular weights of poly(ethylene glycol) (PEG) as well as dodecane, polycaprolactone, and poly(butyl acrylate) were grafted to the CNC surface. With PEG-grafted nanoparticles, grafting densities of 0.47 chains nm^{-2} and 0.10 chains nm^{-2} were achieved with 2,000 and 10,000 g mol^{-1} polymer chains respectively, both of which represent significant improvements over previous reports for solution-based PEG grafting onto CNCs.

1. Introduction

Cellulose nanocrystals (CNCs) have become an attractive, sustainable additive to provide mechanical reinforcement in polymeric materials. These bio-derived nanorods, which have dimensions of roughly 10 nm in width and 100-500 nm in length, are directly extracted from cellulosic biomass and have shown outstanding reinforcement capabilities when used as fillers in composites.[1] A key challenge in accessing such nanocomposites is the ability to achieve a uniform dispersion of CNCs within a given matrix and this has limited the use of CNCs to a relatively narrow range of applications.[2] The poor dispersion of CNCs in many solvents or solid polymer matrices arises from the numerous hydroxyl functional groups present on the surface of the particles that make them very hydrophilic and capable of forming inter-particle hydrogen bonds. Since many potential host polymers are hydrophobic, the inter-particle interactions between CNCs cause the formation of agglomerates, significantly impeding their ability to reinforce the host matrix.[3]

Surface modification of CNCs has been widely explored to overcome these dispersion issues and promote more homogenous mechanical reinforcement of the material.[4] Some surface modification routes utilize these interactions to physisorb or electrostatically adsorb surfactants or polymers onto CNCs.[5–8] Additionally, surface modification can be achieved through covalent attachment of small molecules via different chemical reactions such as esterification, etherification, silylation, amidation, and urethanization.[9–11] A third, widely-employed method of CNC surface modification involves the covalent grafting of polymer chains.[12,13] In addition to improving dispersion, such polymer-grafted nanoparticles can also show enhanced interfacial adhesion between the filler and the polymer matrix through entanglements or other matrix-filler interactions.[13] Depending on the grafted polymer conformation, which is a function of the polymer molecular weight and grafting density, these interactions can greatly aid both the processing and properties of the resulting nanocomposite materials.[14,15]

Different pathways have been developed to graft polymers on the surface of CNCs, including "grafting-to", "grafting-from", and "grafting-through" approaches, among others.[16–18] The "grafting-from" approach relies on covalent attachment of an initiator on the CNC surface and allows for initiation of the polymerization directly from the nanoparticle surface.[17] The advantages of "grafting-from" include synthetic simplicity and the ability to achieve relatively high surface grafting densities of 0.1 to 0.4 chains nm^{-2}, even for high molecular weight polymers (greater than 10,000 g mol^{-1}).[19] The main drawbacks of "grafting-from" methods are the challenges to characterizing the molecular weight, composition, and surface density of the grafted polymers. Additionally, these are solution-based reactions, which can limit scalability.

Comparatively, "grafting-to" methods typically involve the direct attachment of end-functionalized polymer chains to the surface of the nanocrystals.[20] The benefit of these methods is the ability to attach well-characterized polymer chains to CNCs, allowing for more thorough characterization of grafting density, polymer molecular weight, and brush structure. Surface brush conformation is known to play a significant role in resulting material properties, such as improved ionic conductivity[21] and water transport[22] at higher grafting densities and improved reinforcement potential with semi-dilute brush conformations.[15,23] Unfortunately, "grafting-to" functionalization relies on sequential attachment of polymer chains on the CNC surface. As the surface is populated, unreacted chains in solution can be sterically hindered from reacting with the surface, which can limit grafting density.

Additionally, the most common "grafting-to" methods, which include carbodiimide coupling,[24] epoxy ring opening,[25] and isocyanate-mediated grafting,[26] are all typically performed in solution (most commonly in water and DMF), once again limiting the use of these methods to lab-scale.[13,27] This use of potentially toxic solvents during the grafting reaction for both "grafting-to" and "grafting-from" techniques is antithetical to the core purpose of using sustainable nanoparticles. Thus, it is paramount to find more industrially relevant routes toward functionalization of CNCs that can achieve high grafting density with a range of polymers and molecular weights while preserving the renewable character of the nanoparticles.

One promising "grafting-to" method that has industrial relevance is the use of isocyanate moieties that can react with the hydroxyl groups on CNCs to form urethane linkages. This reaction is ubiquitous in the polyurethane industry[28] and has also been used to functionalize CNCs.[9] One limitation of this method when used with CNCs is the hygroscopic nature of the nanoparticles. Isocyanates can react with any water present, releasing CO_2 and degrading into an amine, which can further react with other isocyanates, consuming the reactant before it is able to attach to a CNC surface. One approach to overcome this loss is using a significant excess of isocyanate to counter the water carried by CNCs.[29] An alternative approach that is commonly used in industry, particularly for waterborne polyurethanes, is the use of blocked isocyanates.[30] Such blocked isocyanates can dissociate at elevated temperatures to release the blocking group, regenerating the isocyanate to react with an appropriate hydroxyl or other nucleophilic moiety. For example, Chowdhury et al. utilized blocked isocyanate chemistry to incorporate CNCs into waterborne polyurethane coatings.[31] One class of blocked isocyanate is the hindered urea (HU), where the isocyanate is reacted with a bulky amine compound. Hindered urea moieties are dynamic bonds and have a range of dissociation temperatures depending on the bulkiness of the amine blocking group.[32,33]

In this work, a solvent-free "grafting-to" method is reported. By taking advantage of dynamic covalent HU chemistry, an isocyanate-terminated polymer is generated in-situ (**Figure 1a**), which can subsequently react with surface hydroxyl groups to form a urethane bond, thus functionalizing the CNCs (**Figure 1b**). The solvent-free nature of this reaction makes the technique more environmentally friendly and improves the scalability of the reaction since most industrial processes are conducted in the melt. This study first demonstrates the viability of the concept with model reactions, then translates the developed functionalization process toward the modification of CNCs with a range of polymers.

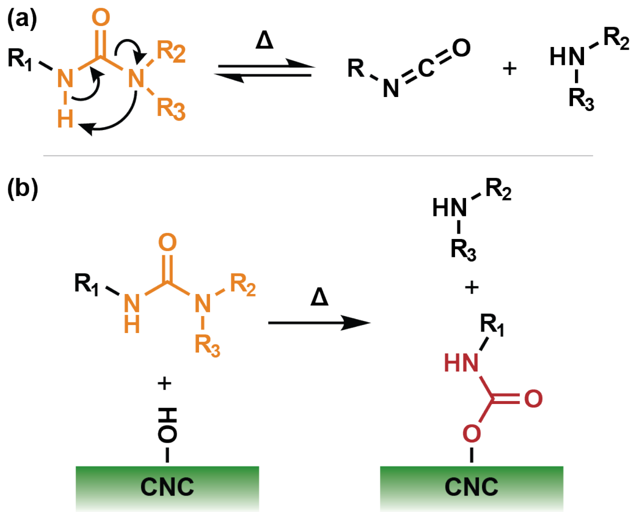

Figure 1. **(a)** Schematic of a dynamic hindered urea motif and its dissociation into an isocyanate and secondary amine, and **(b)** a schematic of the reaction between a dynamic hindered urea and hydroxyl groups on the surface of cellulose nanocrystals, forming a urethane on the CNC surface and releasing the secondary amine.

2. Results and discussion

When designing a hindered urea system for grafting onto CNCs, the dissociation temperature of the blocked isocyanate is a key consideration. Depending on surface functionality, CNCs can begin to degrade around 165 °C[34], so the isocyanate must be regenerated below that limit. Depending on the amine group used to block the isocyanate, hindered urea groups can activate between 30 - 200+ °C.[33,35] For this reason, *N-tert*-butylmethylamine was chosen as the blocking group because of its K_{eq} of roughly 90 M^{-1} at 130 °C, which corresponds to about 8 mol.% hindered urea activation.[35] This activation temperature is above room temperature and the boiling point of water to limit premature reactions, but well below the CNC degradation threshold.

2.1. Isolation and Characterization of *c*-CNC-OSO_3 and *c*-CNC-COOH

Following a previously reported procedure,[36] cellulose nanocrystals were isolated from cotton-based cellulose filter paper using sulfuric acid (*c*-CNC-OSO_3) and hydrochloric acid (*c*-CNC-OH) (see the supporting information (SI) for full experimental procedures). Following isolation, the *c*-CNC-OH nanoparticles were treated with (2,2,6,6-tetramethylpiperidin-1-yl)oxyl (TEMPO) to oxidize primary alcohol groups on the CNC surface into carboxylate groups, transforming *c*-CNC-OH into *c*-CNC-COOH. The resulting nanoparticles were freeze-dried for easier handling before full characterization. In brief, atomic force microscopy (AFM) was used to measure the dimensions of the *c*-CNC-COOH to be 170 ± 80 nm in length, 23 ± 5 nm in width, and 10 ± 3 nm in height (**Figures S1a and S1b**). The dimensions of *c*-CNC-OSO_3 were 148 ± 93 nm, 60 ± 10 nm, and 8 ± 3 nm in length, width, and height, respectively (**Figure S2a**). Conductivity titration determined the surface carboxylate density to be 410 ± 60 mmol kg^{-1} (**Figure S1c**) and surface sulfate density to be 285 ± 24 mmol kg^{-1} (**Figure S2b**). Wide angle X-ray scattering (WAXS) measured the crystallinity index to be 0.67 (**Figure S1d**) for *c*-CNC-COOH and 0.85 for *c*-CNC-OSO_3 (**Figure S2c**). Finally, thermogravimetric analysis (TGA) showed a degradation onset ($T_{d,95}$) of 226 °C for *c*-CNC-COOH (**Figure S1e**) and 175 °C for *c*-CNC-OSO_3 (**Figure S2d**).

2.2. Reactions of Alkyl Hindered Ureas with Protected Sugars and CNCs

To study the dissociation temperature of the selected hindered urea component, a series of model experiments were conducted with a hindered urea-terminated alkyl chain. Specifically, dodecyl isocyanate was reacted with *N-tert*-butylmethylamine in toluene to make dodecyl-HU. The dissociation of dodecyl-HU was monitored in the melt over a range of temperatures using *in-situ* Fourier Transform Infrared (FTIR) spectroscopy (**Figure S3a**). Dodecyl-HU was heated from 30 °C to 130 °C in increments of 10 °C, waiting 10 minutes between each increment. During this test, a characteristic isocyanate N=C=O stretching peak at 2270 cm^{-1} began appearing around 100 °C, indicating the dissociation of hindered urea group and the evaporation of the *N-tert*-butylmethylamine (b.p. 69 °C) (**Figure S3b**). The intensity of the isocyanate band continued to increase with temperature up to 130 °C. Concomitantly, the hindered urea C=O stretching band at 1630 cm^{-1} disappeared as a new band appeared at 1654 cm^{-1}, corresponding to C=O stretching of the isocyanate (Figure S3b).

Prior to examining the ability of the dodecyl-HU to react with CNCs, a model experiment was carried out by reacting dodecyl-HU with 1,2:3,4-di-O-isopropylidene-α-Dgalactopyranose (referred to as PG) (**Figure 2a**). PG is a protected galactose derivative with only the primary 5-hydroxyl group available for reaction, which allows for easier characterization of urethane bond formation.[37] Dodecyl-HU and PG were mixed in a 1:1 molar ratio using a minimal amount of acetone. The solvent was removed under high vacuum and the reaction proceeded in the melt at 120 °C for 5 hours. The disappearance of the hindered urea and formation of the urethane compound were monitored by in-situ FTIR (**Figure 2b**), highlighting the disappearance of the urea C=O stretching peak at 1645 cm^{-1} and the concomitant appearance of the urethane C=O stretching peak at 1722 cm^{-1}. It is worthwhile to note that no other significant peaks appear in the carbonyl region, suggesting that this reaction is relatively clean and avoids the formation of side products. Additionally, synthesis was confirmed with ^{1}H NMR after purification (Figure S4).

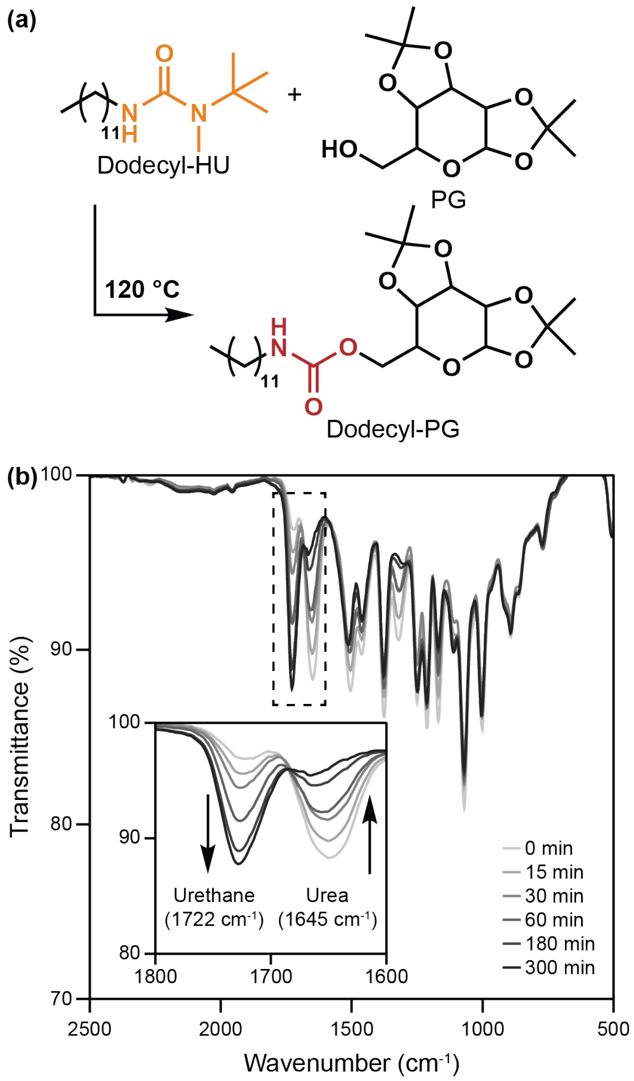

Figure 2. (a) Schematic of the reaction between PG and dodecyl-HU to form a urethane bond and **(b)** the FTIR spectra of the reaction over time, showing the disappearance of the urea peak at 1645 cm^{-1} and the appearance of the urethane peak at 1722 cm^{-1}.

The covalent attachment of dodecyl-HU to CNC was then explored by combining a 2:1 molar ratio of HU to surface alcohol groups on the *c*-CNC-OSO_3 (calculated based on prior literature[15]) in minimal acetone to blend the components (**Figure 3a**). In this initial test, sulfate-functionalized CNCs were selected due to the presence of reactive primary hydroxyl groups as well as charged sulfate surface groups to promote dispersion and mixing.[38] After removing the acetone with vacuum, the bulk mixture was heated to 120 °C for 2 hours to avoid CNC degradation at prolonged times. To characterize the grafting, it was necessary to remove the unreacted dodecyl-HU from the functionalized CNCs, which was achieved by washing the reaction mixture five times with acetone (see SI for full procedure). The resulting *c*-CNC-*g*-dodecane was characterized using FTIR, which showed the appearance of the urethane C=O peak at 1710 cm^{-1} (**Figure 3b**). It is noteworthy that although the broadness of the urethane peak could indicate the formation of side products, such as allophanates,[39] the increased thermal stability of c-CNC-g-dodecane seen in the TGA curve still supports surface modification (Figure S5).While these measurements did not allow for quantification of the dodecyl group surface density, these results confirm a successful reaction between the CNCs and the small molecule hindered urea.

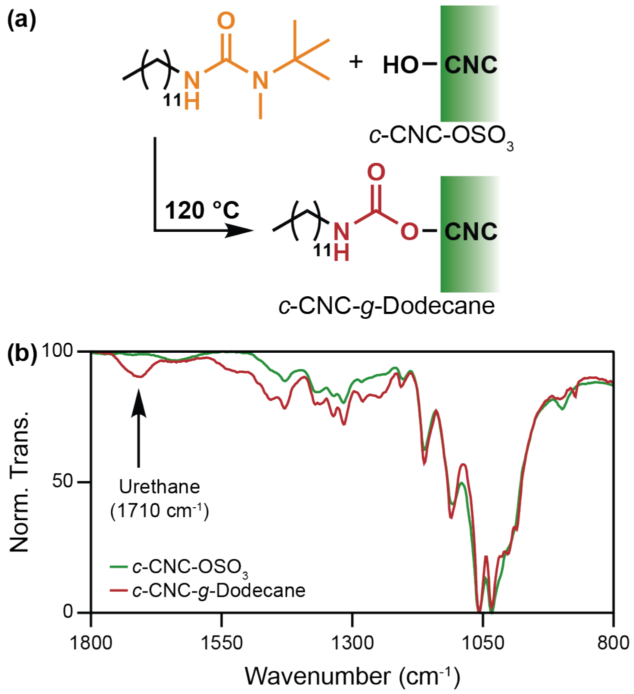

Figure 3. (a) A schematic of the reaction between dodecyl-HU and surface alcohol groups on CNCs and **(b)** FTIR spectra of the resulting purified *c*-CNC-*g*-dodecane, highlighting the appearance of the urethane peak at 1710 cm^{-1}.

Having confirmed that it is possible to functionalize the CNC surface with a small molecule using dynamic hindered urea chemistry in the bulk, the next step was to explore the grafting of polymers onto CNC surfaces using this approach.

2.3. Synthesis and Characterization of Hindered Urea-Terminated Polymers

To demonstrate the versatility of this functionalization method, four polymers were chosen for functionalization onto CNC surfaces: poly(ethylene glycol) at 2,000 and 10,000 g mol^{-1} (PEG_{2k} and PEG_{10k}) as well as polycaprolactone (PCL_{10k}) and poly(butyl acrylate) (PBA_{10k}), both at 10,000 g mol^{-1}. PEG was chosen to allow comparison with previously reported solution-based "grafting-to" chemistries that have been used to synthesize PEG-grafted CNCs,[15] bio-based PCL was chosen to highlight the ability to make fully sustainable nanoparticles, and PBA was chosen to highlight the ability to functionalize and graft polymers synthesized via controlled, living polymerization techniques.

2.3.1. Synthesis and Characterization of PEG-HU and PCL-HU

After purchasing and synthesizing[40] PEG-OH and PCL-OH respectively (see SI for synthetic details), the next step was to create hindered urea-terminated polymers. For simplicity, discussion about synthesis and characterization will focus on PEG_{2k}, but reaction conditions and observations were similar between all PEG and PCL materials. Isocyanate-terminated PEG_{2k} (PEG_{2k}-NCO) was synthesized at 40 °C in dry toluene using an excess of hexamethylene diisocyanate and dibutyltin dilaurate (DBTDL) as catalyst (**Figure 4a**). During the work-up of this intermediate, it was vital to maintain an inert atmosphere and keep the material as cold as possible. Even brief exposure to atmospheric conditions resulted in impurities in the final product. Once the PEG_{2k}-NCO had been reacted with *N*-*tert*-butylmethylamine (Figure 4a), the resulting hindered urea-terminated PEG_{2k} (PEG_{2k}-HU) was much more stable and could be stored at ambient conditions for an extended period. The same phenomena were also observed when synthesizing PEG_{10k}-NCO and PEG_{10k}-HU as well as PCL_{10k}-NCO and PCL_{10k}-HU.

PEG_{2k}-NCO was characterized with FTIR (**Figure 4b**), size exclusion chromatography (SEC) (**Figure S6a**), and ^{1}H NMR (**Figure S6b**) to verify its structure prior to protecting the isocyanate with the secondary amine. Once protected with *N*-*tert*-butylmethylamine, ^{1}H NMR was repeated to confirm the appearance of peaks at 2.81 ppm and 1.39 ppm, corresponding to the methyl and *tert*-butyl groups of the HU, respectively (Figure S6b). Additionally, the appearance of the urea peak at 1631 cm^{-1} in FTIR confirmed successful synthesis (Figure 4b). Shoulders around the urethane peak imply that isocyanate side reactions could be occurring, such as the formation of allophanates and biurets. This is further suggested by the presence of a small peak in the SEC that is roughly double the initial polymer mass (Figure S6a). While the presence of these components would impact the stoichiometry of grafting reactions, their relatively small mass fraction (15 wt.% based on the PEG_{2k}-HU SEC peak) means that these are minor side reactions. Similar characterization was conducted on PEG_{10k}-NCO and -HU as well as PCL_{10k}-NCO and -HU (**Figures S7 and S8**).

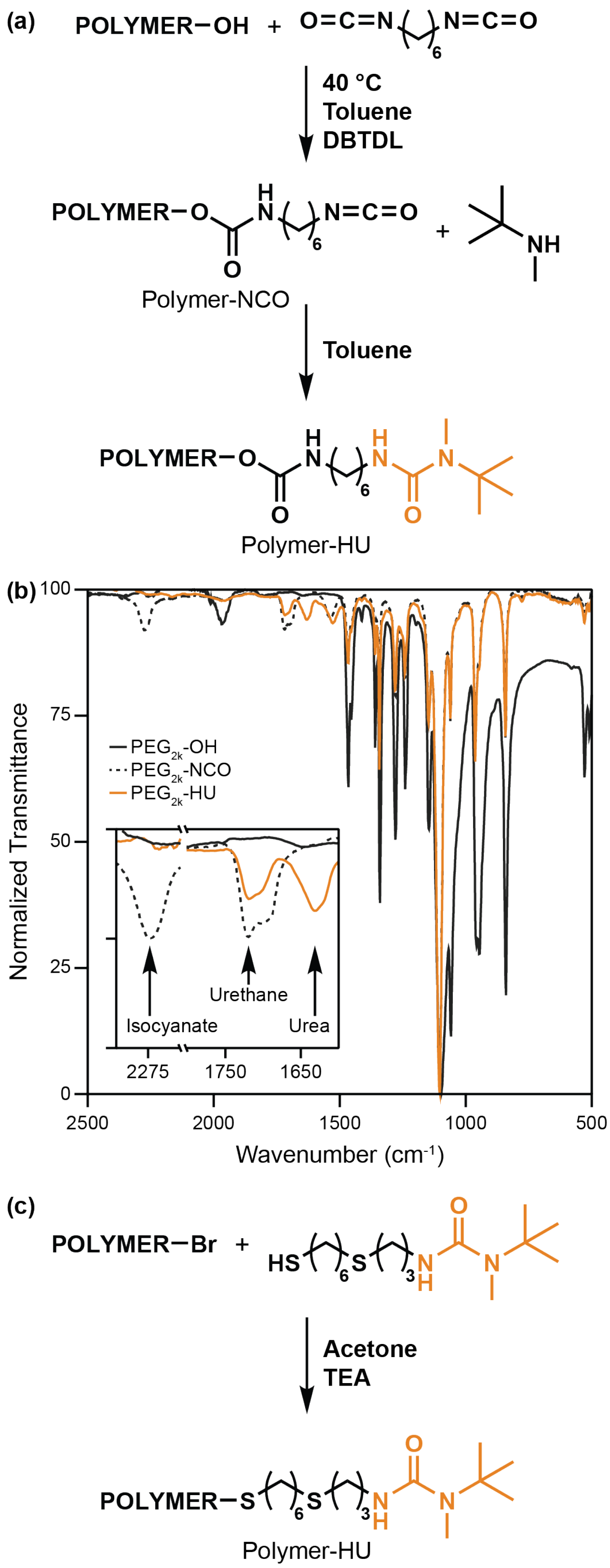

Figure 4. (a) Schematic for the conversion of polymers with alcohol end groups into hindered urea-terminated polymers, **(b)** FTIR spectra of PEG_{2k}-OH, PEG_{2k}-NCO, and PEG_{2k}-HU showing the appearance of the isocyanate peak at 2272 cm^{-1} in PEG_{2k}-NCO and the urea peak at 1631 cm^{-1} in PEG_{2k}-HU, and **(c)** a schematic for the conversion of polymers with bromine end groups into hindered urea-terminated polymers.

2.3.2. Synthesis and Characterization of PBA-HU

Synthesis of bromine-terminated PBA-Br was achieved using Cu(0)-mediated living radical polymerization with ethyl α-bromoisobutyrate as the initiator (**Figure S9**) (see SI for full experimental procedures).[41] To substitute a hindered urea group onto the bromine chain end, a thiol-functionalized hindered urea was synthesized by blocking allyl isocyanate with *N-tert*-butylmethylamine (**Figure S10**). Then, thiol-ene click chemistry was used with an excess of 1,6-hexanedithiol to generate the desired thio-HU small molecule (**Figure S11**). Finally, nucleophilic substitution was conducted between the thio-HU and bromine end group to connect the hindered urea to the polymer chain (**Figure 4c**). After purification of PBA-HU, SEC showed a small shift to shorted retention times, consistent with the substitution of the bromine by the thio-HU moiety (**Figure S9a**). Additionally, ^{1}H NMR showed the appearance of the methyl and tert-butyl group peaks at 2.81 ppm and 1.39 ppm respectively (**Figure S9b**).

2.4. Preparation, Characterization, and Optimization of PEG_{2k}-grafted *c*-CNCs

In prior work, it has been shown that it is possible to quantify the amount of PEG grafted to CNC-COOH using dynamic thermogravimetric analysis.[15] During initial HU-terminated polymer grafting tests using sulfate-functionalized *c*-CNC-OSO_3, it was found that the broader degradation range of the *c*-CNC-OSO_3 (Figure S2d) made quantification of the polymer content on the grafted nanoparticles difficult via TGA. For this reason, grafting to *c*-CNC-COOH with a narrower degradation window (Figure S1e) was adopted, resulting in better separation of cellulose and PEG degradation via thermogravimetry. The key difference between these types of CNC is the presence of the more reactive primary hydroxyl groups on the *c*-CNC-OSO_3, whereas most of the primary alcohols have been converted to carboxylate groups on the *c*-CNC-COOH. However, isocyanates can also react with the secondary alcohols on a sugar unit, albeit at a lower rate.[42]

To prepare for grafting, freeze-dried *c*-CNC-COOH were dispersed in water at a concentration of 5 mg mL^{-1} and solvent exchanged into acetone. Using PEG_{2k} as a preliminary sample, 400 mg (approx. 2.7 mol eq. relative to surface -OH groups) of PEG_{2k}-HU were dissolved in the CNC dispersion per 100 mg of *c*-CNC-COOH. The acetone was then removed under high vacuum at ambient temperature. The resulting powder was melted at 120 °C and stirred for 2 hours under vacuum (120 mbar) to remove the volatile amine and yield *c*-CNC-*g*-PEG_{2k} (**Figure 5a**).

To explore the effects of the amine blocking group on CNC grafting, grafting was also conducted with PEG_{2k}-NCO (**Figure 5b**). Experimentally, the procedure was identical to PEG_{2k}-HU grafting, but was done immediately after PEG_{2k}-NCO preparation to avoid any loss of the isocyanate that could occur from hydrolysis or other side reactions during storage. Grafting was conducted under vacuum on an FTIR thermal stage so that spectra could be gathered *in situ*. The resulting spectra for PEG_{2k}-NCO (**Figure 5c**) highlights the proclivity of the isocyanate to undergo side reactions with large shoulders appearing around 1765 and 1700 cm^{-1} in the grafted sample (Figure 5c inset). These peaks likely correspond to uretdione[43] and allophanate[39] production, respectively. The PEG_{2k}-HU-grafted sample shows notably smaller shoulders (**Figure 5d**). To quantify these differences, the decrease of the isocyanate (2275 cm^{-1}) and urea (1655 cm^{-1}) reactant peaks is plotted against time along with the increase of the product urethane peak (1722 cm^{-1}). In an ideal system, the consumption of reactants should translate directly into product growth, indicating inhibition of any side reactions taking place. For grafting with PEG-NCO (**Figure 5e**), these two curves diverge within the first 30 minutes of the reaction, which suggests that the isocyanate moiety is undergoing side reactions. In contrast, the PEG-HU grafting curves (**Figure 5f**) show a slower, more steady consumption of the hindered urea peak and a corresponding increase in the urethane peak throughout the reaction. This data is consistent with slower, more controlled grafting with the hindered urea relative to the unblocked isocyanate.

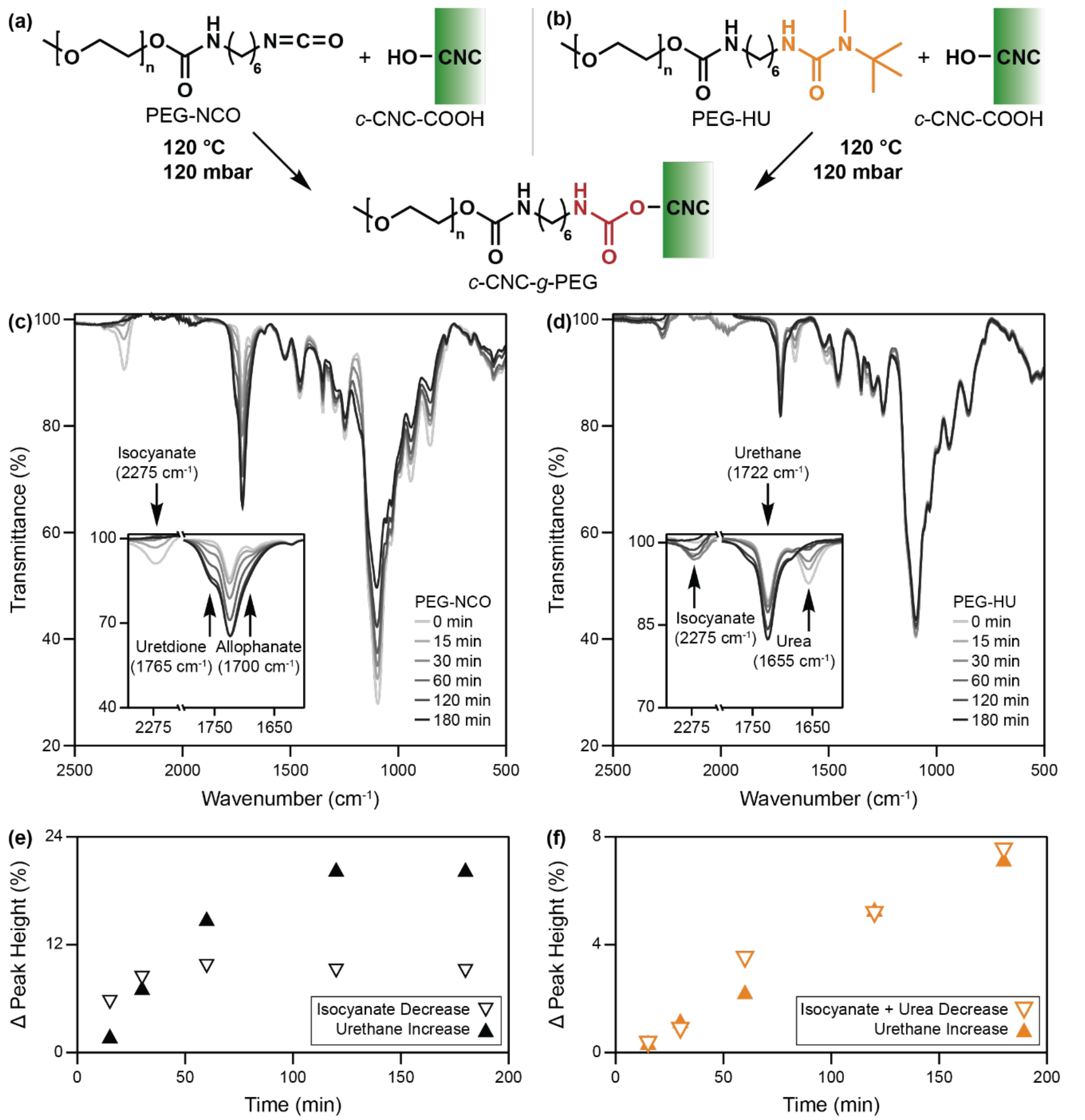

Figure 5. (a) Schematic of grafting PEG-NCO onto the hydroxyl groups of CNCs, **(b)** schematic of grafting PEG-HU onto the hydroxyl groups of CNCs, **(c)** time-resolved FTIR of PEG_{2k}-NCO grafting to *c*-CNC-COOH highlighting the shoulders appearing around the urethane peak, **(d)** time-resolved FTIR of PEG_{2k}-HU grafting to *c*-CNC-COOH with no such shoulders, **(e)** change in reactant (isocyanate) and product (urethane) peak heights plotted against time for PEG_{2k}-NCO grafting, and **(f)** change in reactant (isocyanate + urea) and product (urethane) peak heights plotted against time for PEG_{2k}-HU grafting.

To confirm that the polymer chains were indeed grafted to the CNCs, it is important to remove any unreacted polymer and carry out detailed characterization of the degree of functionalization on the polymer-grafted CNCs. To ensure thorough removal of excess unreacted polymer after surface functionalization, a diagnostic test was done by adding dye-tagged PEG to the reaction after completion and tracking the amount of dye remaining in the product after each wash (**Figure S12**). It was found that the most effective washing method for PEG removal was a 1:1 mixture of acetone:water. After 12 centrifugation and resuspension cycles, no residual dye could be detected in the supernatant, implying that most, if not all, of the non-attached polymer chains had been removed. This strategy was then employed for the removal of untagged free polymer chains in all other samples.

After thorough cleaning, the amount of grafted polymer was measured using high resolution, dynamic TGA. Dynamic TGA is a procedure that slows the heating rate of the experiment whenever a mass loss event is detected, which helps to isolate individual degradation events. This method allowed for enhanced separation of CNC and polymer degradation, allowing for more accurate quantification of polymer content via thermogravimetry (**Figure 6a**).[44] By taking the derivative of the mass loss and interpolating a line between the points at 330 and 400 °C to account for baseline CNC degradation, the PEG mass fraction could be determined via integration of the degradation peak (**Figures 6b and S13**) and used to calculate the surface grafting density based on the crystal structure of cellulose and the CNC dimensions measured via AFM.[15,45]

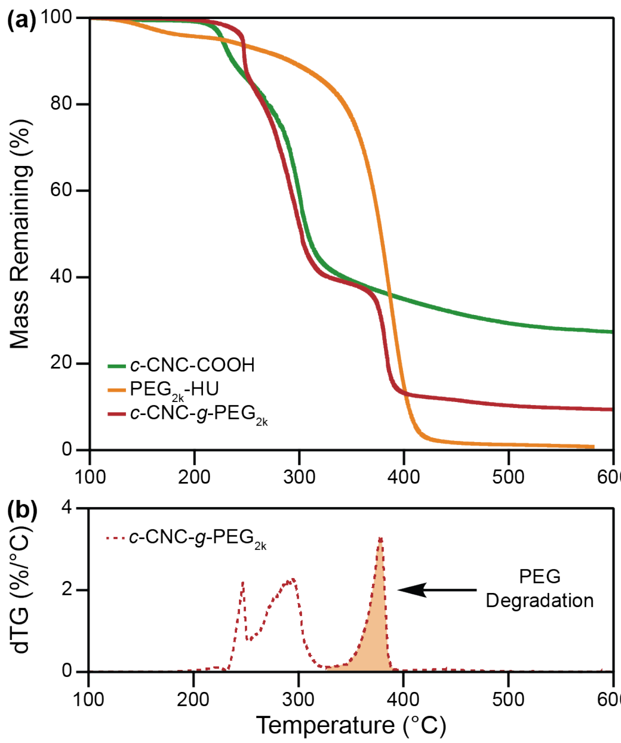

Figure 6. (a) TGA degradation curves of *c*-CNC-COOH, PEG_{2k}-HU, and a characteristic sample of *c*-CNC-*g*-PEG_{2k} and **(b)** the derivative of the *c*-CNC-*g*-PEG_{2k} degradation curve, highlighting the separation of CNC degradation and PEG degradation (shaded).

With characterization established, a series of experiments were done to optimize the reaction conditions for grafting PEG_{2k}-HU to *c*-CNC-COOH by varying the reaction time, reaction temperature, and ratio of polymer to surface hydroxyl groups (**Table 1**). The model reactions discussed earlier helped to define upper and lower limits for these tests, with 2 hours, 120 °C, and 400 mg PEG for every 100 mg *c*-CNC-COOH being considered the baseline conditions. From these studies, two hours was found to be the optimal reaction time, with shorter reactions not allowing for full HU conversion and longer reactions allowing more time for side reactions to reduce grafting density. The optimal reaction temperature was found to be 130 °C, with lower temperatures not activating the hindered urea groups efficiently enough and higher temperatures promoting side reactions.

Table 1. An array of *c*-CNC-*g*-PEG_{2k} grafting reaction conditions and the resulting reaction efficiencies and grafting densities.

c-CNC-COOH [mg]	PEG_{2k}-HU [mg (mol eq.)[a)]]	Time [hr]	Temperature [°C]	Reaction Efficiency [% of chains grafted]	Grafting Density [chains nm^{-2}]
100	400 (2.7)	1.5	120	4.6	0.30
[b)]100	400 (2.7)	2	120	6.6	0.42
100	400 (2.7)	3	120	4.9	0.32
100	400 (2.7)	4	120	2.3	0.14
100	400 (2.7)	2	110	4.7	0.30
[b)]100	400 (2.7)	2	120	6.6	0.42
100	400 (2.7)	2	130	7.4	0.47
100	400 (2.7)	2	140	4.6	0.30
100	100 (0.7)	2	120	15.4	0.25
100	200 (1.4)	2	120	13.8	0.44
[b)]100	400 (2.7)	2	120	6.6	0.42
100	800 (5.4)	2	120	2.8	0.36
100	1600 (10.9)	2	120	1.2	0.30

[a)]molar equivalent relative to surface alcohol groups on the *c*-CNC-COOH, [b)]denotes the same baseline data, repeated for clarity

While it was expected that grafting efficiency would decrease as the ratio of polymer to *c*-CNC-COOH mass increased, it was found that the grafting density plateaued above 200 mg of PEG_{2k}-HU. It is possible that the higher ratio of polymer chains results in an increased concentration of isocyanate groups that can react with each other rather than the CNC surface.

Additionally, steric bulk at the CNC surface may provide a physical limit as more polymer chains attach to the nanoparticles. By reducing the polymer:CNC ratio further to 1:1 by mass, too few polymer chains are present in the system, causing grafting density to be reduced from 0.44 to 0.25 chains nm^{-2}. In fact, varying the polymer:CNC mass ratio allows access to *c*-CNC-*g*-PEG_{2k} with grafting densities that range from 0.25 to 0.44 chains nm^{-2}. It is worth noting that the reaction efficiency (polymer grafted vs. polymer added to the reaction) is better at lower polymer:CNC mass ratios. The optimized reaction conditions for PEG_{2k} grafting (1.4 eq. of polymer relative to surface hydroxyl groups, 2 hour reaction time, and 130 °C) were used to graft all other polymers to the CNC surface to allow for comparison.

2.5. Results and Analysis of Grafting with a Variety of Polymers

To explore the versatility of this technique, grafting was also carried out with HU-terminated PEG_{10k}, PCL_{10k}, and PBA_{10k} in addition to PEG_{2k} with the established optimized conditions. For PCL and PBA-grafted CNCs, the cleaning washes were done with THF, which is a good solvent for both polymers.

It was not possible to determine the amount of PCL in the *c*-CNC-*g*-PCL_{10k} samples using dynamic TGA as PCL degradation could not be deconvoluted from CNC degradation. Thus, an FTIR calibration curve was created by mixing varying ratios of PCL and CNCs and measuring the relative intensity of the 1724 cm^{-1} peak in the normalized spectra, corresponding to the carbonyl group in the PCL repeat unit (**Figure 7**). When plotted against PCL content, the peak heights generated a linear relation that could be used to estimate grafted PCL content (Figure 7 inset). For PBA, both dynamic TGA and FTIR calibration curves were used to quantify the grafted polymer content, and both methods corroborated each other (**Figures S14 and S15**).

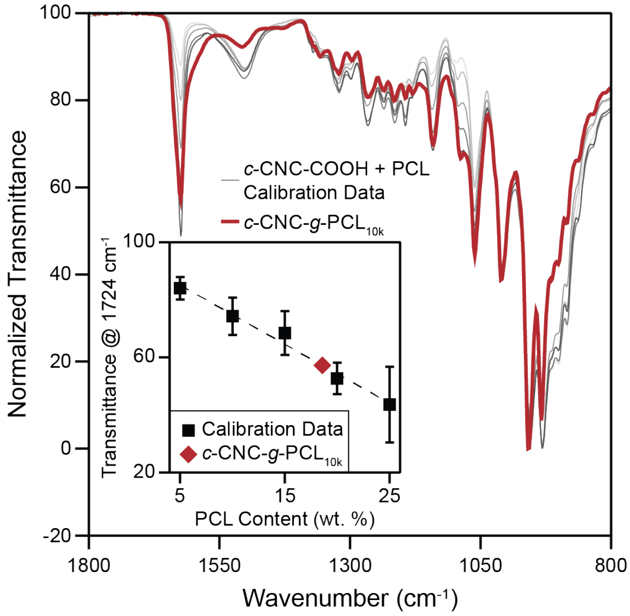

Figure 7. FTIR data for *c*-CNC-COOH mixed with PCL_{10k}-OH at various ratios along with the resulting calibration curve (inset) with the polymer-grafted *c*-CNC-*g*-PCL_{10k} overlayed on both.

Table 2. Grafting results for a variety of polymers onto *c*-CNC-COOH using optimized grafting conditions.

Sample	**Polymer Mass Fraction [wt. %]**	**Grafting Density [chains/nm^2]**
c-CNC-*g*-PEG_{2k}	22.4[a)]	0.46
c-CNC-*g*-PEG_{10k}	24.5[a)]	0.10
c-CNC-*g*-PCL_{10k}	18.6[b)]	0.07
c-CNC-*g*-PBA_{10k}	8.7[b)]	0.03

[a)]measured via dynamic TGA, [b)]measured via FTIR calibration curve

The results for grafting all polymers with the optimized conditions can be seen in **Table 2**. Putting these results in the context of other grafting methods, prior work from Rowan and coworkers used peptide coupling in DMF to access PEG-grafted CNCs.[15] With PEG_{2k}, the best reaction conditions resulted in a grafting density of 0.33 chains nm^{-2}. This work observed a grafting density of 0.46 chains nm^{-2} using the optimized conditions, which is notably higher than the grafting density achieved in solution. It is, of course, important to note that the isocyanates can react with the 2- and 3-hydroxyl groups on the cellulose unit, whereas only the primary 6-hydroxyl can react with the amine during peptide coupling. It is possible to use the hindered urea grafting approach to replicate the solution grafting density reported in this prior literature using half as much polymer reactant by mass.

For PEG_{10k} grafting, the resulting grafting density was 0.10 chains nm^{-2}, which is lower than the PEG_{2k}-grafted sample presumably on account of the steric bulk of the larger polymer chains, as seen in prior work[15]. Compared to the highest solution grafting density results of 0.07 chains nm^{-2} for PEG_{10k}, the hindered urea grafting method developed herein is able to achieve greater grafting densities than solution-based grafting methods.[15] Composites with PLA were prepared for the PEG_{2k} and PEG_{10k}-grafted CNCs and were shown to exhibit properties similar to those seen in prior solution-grafted CNC composites (**Figure S16**).[15]

Based on the FTIR calibration curve for *c*-CNC-*g*-PCL_{10k}, the calculated grafting density of 0.07 chains nm^{-2} is slightly lower than the PEG_{10k} grafting density. While the different polymer structures make these results difficult to compare, it is hypothesized that the reduced flexibility of the polycaprolactone chain (Kuhn length b = 10.0 Å for PCL[46] vs. b = 7.6 Å for PEG[47]) likely increases the steric hinderance at the nanoparticle surface, resulting in fewer polymer chains finding a reactive site on the CNC. Nearly all PCL-grafted CNCs in literature are synthesized via ring opening polymerization from the CNC surface, which is a technique that makes it difficult to characterize the grafted chain length or density. As an elementary comparison, a few reports have used FTIR to characterize their PCL-grafted CNCs and the relative intensity of the 1724 cm^{-1} peak corresponding to the carbonyl in the PCL backbone is roughly similar to the relative intensity observed here (Figure 7), suggesting that the PCL content of the resulting nanoparticles is competitive with grafting-from techniques.[11,48,49]

Finally, PBA_{10k} grafting resulted in 0.03 chains nm^{-2}, which is notably lower than the PEG_{10k} and PCL_{10k} counterparts. This reduction in grafting density has been attributed to a further increase in the steric bulk from the butyl pendant group, as highlighted by a further increase in the Kuhn length to b = 17.1 Å for PBA[50]. Additionally, the more hydrophobic nature of this polymer may hinder mixing during the melt grafting process, further limiting surface functionalization. Regardless, the FTIR and TGA traces (**Figures S14 and S15**) show clear evidence of grafting, and the synthesis method is potentially applicable to a wide range of bromine-terminated polymers.

3. Conclusions

Taking inspiration from the polyurethane industry, a method has been developed for the melt-functionalization of cellulose nanocrystals. By installing dynamic hindered urea moieties on the end of polymer chains, isocyanate groups were formed in-situ in the bulk. The isocyanate groups generated were able to react with surface hydroxyl groups on the CNCs, linking the polymer to the nanoparticle via a urethane linkage. The efficacy of the reaction was verified with a model small molecule system before being optimized with hindered urea-terminated PEG_{2k} chains on cotton-based, TEMPO-oxidized CNCs. Compared to the unblocked isocyanate, the hindered urea-functionalized polymer chains showed fewer side reactions, emphasizing the increased synthetic control afforded by the blocked system. The resulting polymer-grafted nanoparticles exhibited grafting densities that were superior to solution-based functionalization methods without the need for harmful solvents during the grafting reaction. Finally, the versatility of this method was highlighted by grafting CNC surfaces with hindered urea-terminated dodecane, PEG_{10k}, PCL_{10k}, and PBA_{10k}. Each of the resulting polymer-grafted nanoparticles showed polymer contents that were competitive with literature. Sustainable and efficient processing are crucial characteristics for polymer-grafted CNC to achieve commercial success going forward, and this method advances both of those metrics while achieving strong grafting densities with a range of polymers.

4. References

[1] C. Calvino, N. Macke, R. Kato, S. J. Rowan, *Prog. Polym. Sci.* **2020**, *103*, 101221.

[2] A. Dufresne, *Int. Polym. Process.* **2012**, *27*, 557.

[3] R. J. Moon, A. Martini, J. Nairn, J. Simonsen, J. P. Youngblood, *Chem. Soc. Rev.* **2011**, *40*, 3941.

[4] S. Chanda, D. S. Bajwa, *Rev. Adv. Mater. Sci.* **2021**, *60*, 325.

[5] Y. Habibi, L. A. Lucia, O. J. Rojas, *Chem. Rev.* **2010**, *110*, 3479.

[6] N. Dhar, D. Au, R. C. Berry, K. C. Tam, *Colloids Surfaces A Physicochem. Eng. Asp.* **2012**, *415*, 310.

[7] H. R. Paul, M. K. Bera, N. Macke, S. J. Rowan, M. V. Tirrell, *ACS Nano* **2024**, *18*, 1921.

[8] S. Eyley, W. Thielemans, *Nanoscale* **2014**, *6*, 7764.

[9] J. C. Natterodt, A. Petri-fink, C. Weder, J. O. Zoppe, *Chimia (Aarau).* **2017**, *71*, 376.

[10] Y. Habibi, *Chem Soc Rev* **2014**, *43*, 1519.

[11] S. Wohlhauser, G. Delepierre, M. Labet, G. Morandi, W. Thielemans, C. Weder, J. O. Zoppe, *Macromolecules* **2018**, *51*, 6157.

[12] S. A. Kedzior, J. O. Zoppe, R. M. Berry, E. D. Cranston, *Curr. Opin. Solid State Mater. Sci.* **2019**, *23*.

[13] E. Lizundia, E. Meaurio, J. L. Vilas, in *Multifunct. Polym. Nanocomposites Based Cellul. Reinf.*, Elsevier, **2016**, pp. 61–113.

[14] N. Macke, C. M. Hemmingsen, S. J. Rowan, *J. Polym. Sci.* **2022**, *60*, 3318.

[15] L. Geurds, J. Lauko, A. E. Rowan, N. Amiralian, *J. Mater. Chem. A* **2021**, *9*, 17173.

[16] S. Minko, in *Polym. Surfaces Interfaces*, Springer, **2008**, pp. 215–234.

[17] P. V. Kelly, S. Shams Es-haghi, M. E. Lamm, K. Copenhaver, S. Ozcan, D. J. Gardner, W. M. Gramlich, *ACS Appl. Polym. Mater.* **2023**, *5*, 3661.

[18] S. Wohlhauser, C. Rader, C. Weder, *Biomacromolecules* **2022**, *23*, 699.

[19] B. Zdyrko, I. Luzinov, *Macromol. Rapid Commun.* **2011**, *32*, 859.

[20] R. Kato, J. H. Lettow, S. N. Patel, S. J. Rowan, *ACS Appl. Mater. Interfaces* **2020**, *12*, 54083.

[21] H. R. Paul, M. V. Tirrell, S. J. Rowan, *ACS Appl. Nano Mater.* **2024**, *7*, 4210.

[22] J. H. Lettow, H. Yang, P. F. Nealey, S. J. Rowan, *Macromolecules* **2021**, *54*, 10594.

[23] F. Azzam, L. Heux, J.-L. Putaux, B. Jean, *Biomacromolecules* **2010**, *11*, 3652.

[24] E. Kloser, D. G. Gray, *Langmuir* **2010**, *26*, 13450.

[25] A. Pei, J.-M. Malho, J. Ruokolainen, Q. Zhou, L. A. Berglund, *Macromolecules* **2011**, *44*, 4422.

[26] D. Viet, S. Beck-Candanedo, D. G. Gray, *Cellulose* **2007**, *14*, 109.

[27] J. O. Akindoyo, M. D. H. Beg, S. Ghazali, M. R. Islam, N. Jeyaratnam, A. R. Yuvaraj, *RSC Adv.* **2016**, *6*, 114453.

[28] H. Abushammala, *Polymers (Basel).* **2019**, *11*, 1.

[29] Z. W. Wicks, *Prog. Org. Coatings* **1975**, *3*, 73.

[30] R. A. Chowdhury, C. M. Clarkson, S. Shrestha, S. M. El Awad Azrak, M. Mavlan, J. P. Youngblood, *ACS Appl. Polym. Mater.* **2020**, *2*, 385.

[31] Q. Zhang, S. Wang, B. Rao, X. Chen, L. Ma, C. Cui, Q. Zhong, Z. Li, Y. Cheng, Y. Zhang, *React. Funct. Polym.* **2021**, *159*, 104807.

[32] H. Ying, Y. Zhang, J. Cheng, *Nat. Commun.* **2014**, *5*, 3218.

[33] O. M. Vanderfleet, M. S. Reid, J. Bras, L. Heux, J. Godoy-Vargas, M. K. R. Panga, E. D. Cranston, *Cellulose* **2019**, *26*, 507.

[34] L. Zhang, S. J. Rowan, *Macromolecules* **2017**, *50*, 5051.

[35] A. M. Weiss, N. Macke, Y. Zhang, C. Calvino, A. P. Esser-Kahn, S. J. Rowan, *ACS Biomater. Sci. Eng.* **2021**, *7*, 1450.

[36] A. Gille, M. Hiersemann, *Org. Lett.* **2010**, *12*, 5258.

[37] K. Oksman, Y. Aitomäki, A. P. Mathew, G. Siqueira, Q. Zhou, S. Butylina, S.

Tanpichai, X. Zhou, S. Hooshmand, *Compos. Part A Appl. Sci. Manuf.* **2016**, *83*, 2.

[38] E. Delebecq, J. Pascault, B. Boutevin, F. Ganachaud, *Chem. Rev.* **2013**, *113*, 80.

[39] B. G. G. Lohmeijer, R. C. Pratt, F. Leibfarth, J. W. Logan, D. A. Long, A. P. Dove, F. Nederberg, J. Choi, C. Wade, R. M. Waymouth, J. L. Hedrick, *Macromolecules* **2006**, *39*, 8574.

[40] A. Anastasaki, V. Nikolaou, G. Nurumbetov, P. Wilson, K. Kempe, J. F. Quinn, T. P. Davis, M. R. Whittaker, D. M. Haddleton, **2016**, DOI 10.1021/acs.chemrev.5b00191.

[41] L. Nagy, B. Vadkerti, G. Batta, P. P. Fehér, M. Zsuga, S. Kéki, *New J. Chem.* **2019**, *43*, 15316.

[42] J. Hu, Z. Chen, Y. He, H. Huang, X. Zhang, *Res. Chem. Intermed.* **2017**, *43*, 2799.

[43] K. Mohomed, *TA Instruments* **2016**, 122.

[44] S. Elazzouzi-Hafraoui, Y. Nishiyama, J.-L. Putaux, L. Heux, F. Dubreuil, C. Rochas, *Biomacromolecules* **2008**, *9*, 57.

[45] D. Herrera, J.-C. Zamora, A. Bello, M. Grimau, E. Laredo, A. J. Müller, T. P. Lodge, *Macromolecules* **2005**, *38*, 5109.

[46] L. J. Fetters, D. J. Lohse, D. Richter, T. A. Witten, A. Zirkel, *Macromolecules* **1994**, *27*, 4639.

[47] C. Tian, S. Y. Fu, Q. J. Meng, L. A. Lucia, *Cellulose* **2016**, *23*, 2457.

[48] Q. Huang, J. Huang, P. R. Chang, *Wuhan Univ. J. Nat. Sci.* **2014**, *19*, 117.

[49] C. Fraschini, G. Chauve, J. Bouchard, *Cellulose* **2017**, *24*, 2775.

[50] A. Anastasaki, V. Nikolaou, G. Nurumbetov, P. Wilson, K. Kempe, J. F. Quinn, T. P. Davis, M. R. Whittaker, D. M. Haddleton, *Chem. Rev.* **2016**, *116*, 835.

[51] A. D. French, *Cellulose* **2014**, *21*, 885.

[52] S. Park, J. O. Baker, M. E. Himmel, P. A. Parilla, D. K. Johnson, *Biotechnol. Biofuels* **2010**, *3*, 1.

Supporting Information

Supporting Information is available from the Wiley Online Library or from the author.

Acknowledgements

Z. Oluz and N. Macke contributed equally to this work. Materials, Methods, and Instrumentation details can be found in the supporting information. The authors gratefully acknowledge financial support through the National Science Foundation (NSF) Center for Sustainable Polymers (CSP) (CHE-1901635) and the Swiss National Science Foundation (SNSF) (P2FRP2_181437). Parts of this work utilized the University of Chicago Materials Research Science and Engineering Center (NSF DMR-2011854), the University of Chicago NMR Facility, the University of Chicago Soft Matter Characterization Facility, and the University of Chicago X-ray facilities.

Received: ((will be filled in by the editorial staff))
Revised: ((will be filled in by the editorial staff))
Published online: ((will be filled in by the editorial staff))

ToC Entry:

Dynamic hindered urea functionality has been used to graft a range of polymers onto cellulose nanocrystals at various molecular weights. By thermally dissociating the hindered urea, an isocyanate group is generated *in-situ* that can then react with surface hydroxyl groups on the nanocrystals. The grafting reaction is done in the melt, without the need for toxic solvents and the resulting polymer-grafted nanoparticles exhibit relatively high surface grafting densities.

Z. Oluz†, N. Macke†, S. Candelaria, A. Ambus, A. Zemborain, C. S. Udemgba, A. M. Weiss, C. Calvino*, S. J. Rowan*

Melt-Functionalization of Cellulose Nanocrystals using Dynamic Hindered Ureas

ToC figure:

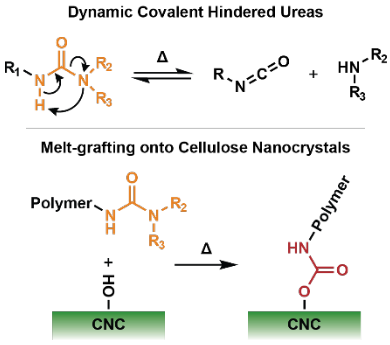

Supporting Information

Melt-Functionalization of Cellulose Nanocrystals using Dynamic Hindered Ureas

*Zehra Oluz†, Nicholas Macke†, Céline Calvino†, Sarah Candelaria, Abrianna Ambus, Aurora Zemborain, Chinwe S. Udemgba, Adam M. Weiss, Stuart J. Rowan**

1. Materials, Methods, and Instrumentation

1.1. Materials

If not specified otherwise, all compounds and solvents were used as received, without further purification. Hydrochloric acid (HCl), sodium bromide (NaBr), sodium hypochlorite (NaOCl), D-(+)-galactose, sulfuric acid, dodecyl isocyanate, *N-tert*-butylmethylamine, methoxy-poly(ethylene glycol) (2,000 g/mol and 10,000 g/mol, PEG_{2k}-OH and PEG_{10k}-OH), hexamethylene diisocyanate, dibutyltin dilaurate (DBTDL), disperse orange 3 (DO3), benzyl alcohol, 1,5,7-Triazabicyclo[4.4.0]dec-5-ene, ε-caprolactone, ethyl α-bromoisobutyrate (EBiB), butyl acrylate, tris[2-(dimethylamino)ethyl]amine (Me_6TREN), copper (II) bromide ($CuBr_2$), allyl isocyanate, 2,2-dimethoxy-2-phenylacetophenone (DMPA), triethylamine (TEA) and chloroform-d were all purchased from Sigma-Aldrich. Whatman filter paper, sodium hydroxide (NaOH), sodium carbonate, copper (0) wire, basic alumina, neutral alumina, and all solvents, acetone, toluene, hexanes, dimethyl sulfoxide (DMSO), diethyl ether, chloroform, tetrahydrofuran (THF), dichloromethane (DCM), ethyl acetate, and N,N-dimethylformamide (DMF), were purchased from Fisher Scientific. (2,2,6,6-tetramethylpiperidin-1-yl)oxyl (TEMPO) was purchased from Ambeed, poly-(L)-lysine was purchased from Ted Pella, 1,6,-hexanedithiol was purchased from Oakwood Chemical, and PLA 4060D was kindly provided by NatureWorks.

1.2. Methods

1.2.1. Preparation of *c*-CNC-OSO_3

10 g of Whatman Number 1 Grade Filter Paper were cut into small pieces, poured into 500 mL deionized water, and blended until formation of a pulp. The CNC-pulp solution was then placed into an ice bath and 280 mL of concentrated sulfuric acid (98 %) was slowly added under stirring. During the addition, the temperature of the reaction was maintained below 35°C. After complete addition, the mixture was heated to 45 °C and stirred for 5 h. The mixture was then cooled to room temperature and filtered through a fine-fritted glass filter. The CNCs were centrifuged at 8000 rpm and resuspended in water ~5 times until the supernatant reached a neutral pH. Finally, the thoroughly washed material was suspended in DI and freeze-dried to yield *c*-CNC-OSO_3^- in fluffy powder form (7.6 g).

1.2.2. Preparation of *c*-CNC-OH

10 g of Whatman Number 1 Grade Filter Paper were cut into small pieces, mixed with 500 mL deionized water, and blended into a uniform pulp. In a 2 L round bottom flask, 75 mL of concentrated HCl was combined with 225 mL of DI water and heated to 100 °C. Once at temperature, the CNC-pulp solution was added to the HCl solution and stirred for 90 minutes. The mixture was then filtered through fine-fritted glass filter before resuspending the *c*-CNC-OH in DI water. The CNCs were centrifuged at 8000 rpm and resuspended in water ~5 times until the supernatant reached neutral pH. Finally, the thoroughly washed material was suspended in DI water and freeze-dried to yield *c*-CNC-OH in fluffy powder form (7 g).

1.2.3. Preparation of *c*-CNC-COOH via TEMPO Oxidation

TEMPO oxidation of *c*-CNC-OH was conducted based on a prior literature report.[51] In brief, 7 g of *c*-CNC-OH were dispersed in 700 mL of DI water and dispersed with probe sonication. To the dispersed CNCs, pre-dissolved TEMPO (0.109 g, 0.7 mmol), NaBr (0.306 g, 3.5 mmol), and NaOCl (14.08 mL, 210 mmol) were added. The pH was adjusted to 10-10.5 and maintained in that range using 1 M NaOH for 2 hours, or until the pH stopped decreasing. Once the reaction was complete, the solution was filtered through fine-fritted glass filter before resuspending the *c*-CNC-COOH in DI water. The CNCs were centrifuged at 8000 rpm and resuspended in water

~5 times. Finally, the thoroughly washed material was suspended in DI water and freeze-dried to yield *c*-CNC-COOH as a fluffy white powder (6 g).

1.2.4. Determination of Surface Carboxylate Concentration

To determine the carboxylate content of the isolated and oxidized *c*-CNC-COOH, conductivity titration was performed with a pH probe by recording conductivity and pH following dropwise addition of 0.01M NaOH. The resulting conductivity data was plotted against the volume of added NaOH and the weak acid plateau was used to determine the concentration of carboxylates on the surface of the CNCs. The functional group density was determined using the following equation:

$$Carboxylate\ Density\ \left(\frac{mol}{kg}\right) = \frac{Concentration\ \times\ Volume_{plateau}}{Mass\ (kg)}$$

To convert from surface concentration (mol/g) to surface density (groups/nm^2), the calculated value is multiplied by 3.21, which was calculated based on the crystal structure of cellulose Iβ as well as the CNC dimensions measured via AFM.[15] For example, a measured surface concentration of 0.37 mol/kg equates to 1.2 groups/nm^2.

1.2.5. Synthesis of the Isopropylidene-Protected D-galactose (PG)

The isopropylidene protection of D-(+)-galactose was prepared following a previously reported procedure.[37] D-(+)-galactose (5 g, 27.7 mmol, 1 eq) was dissolved in acetone (185 mL) and the solution was put in an ice bath. Concentrated sulfuric acid (98%) was added dropwise into the mixture (5.5 mL, 1.1 mL/g). The reaction mixture was then stirred at room temperature for 5 h and neutralized with a solution of sodium carbonate until reaching a pH of 7. The resulting white precipitate was filtered and washed with acetone. The filtrate was collected and dried under high vacuum to remove residual solvent and yield the protected galactose (PG) as a light-yellow oil. ^{1}H NMR (400 MHz, $CDCl_3$) δ 5.56 (d, J = 5.0 Hz, 1H), 4.61 (dd, J = 8.0, 2.5 Hz, 1H), 4.33 (dd, J = 4.92, 2.63 Hz, 1H), 4.27 (dd, J = 8.1, 1.7 Hz, 1H), 3.90 – 3.80 (m, 2H), 3.72 (dd, J = 10.8, 3.5 Hz, 1H), 1.52 (s, 3H), 1.45 (s, 3H), 1.33 (s, 6H).

1.2.6. Synthesis of alkyl end-functionalized hindered urea (Dodecyl-HU)

Dodecyl isocyanate (1.14 mL, 5.3 mmol, 1eq) and *N-tert*-butylmethylamine (0.65 mL, 5.5 mmol, 1.02eq) were solubilized in dry toluene (100 mL). The mixture was stirred at room temperature for 6 h. The resulting precipitate was filtered, thoroughly washed with hexanes, and dried under high vacuum to yield dodecyl-HU as a white powder. ^{1}H NMR (400 MHz, $CDCl_3$) δ 4.22 (br, 1H), 3.17 (dt, J = 7.5, 5.6 Hz, 2H), 2.81 (s, 3H), 1.48 (t, J = 7.3 Hz, 3H), 1.39 (s, 9H), 1.34 – 1.20 (m, 18H), 0.87 (t, J = 6.8 Hz, 3H).

1.2.7. Procedure for PG and Docedyl-HU model reaction in melt

In a desired ratio, PG and dodecyl-HU compounds were dissolved in a small vial using a minimal amount of acetone (ca. 1-2 mL). A final weight of 200 mg of compound was targeted, to ensure enough material for analysis. The solvent was removed under high pressure vacuum overnight to yield a dried solid powder. The powder was then heated to 120 °C and stirred in ambient atmosphere for 8 h. The experiment was tracked with in-situ FTIR, focusing on the urea and urethane peaks at 1645 and 1722 cm^{-1}, respectively. The resulting compound was precipitated in cold hexanes and dried under high vacuum to obtain a white powder before being characterized with ^{1}H NMR. ^{1}H NMR (400 MHz, $CDCl_3$): δ = 5.54 (d, 1H), 4.77 (br, 1H), 4.60 (d, 1H), 4.31 (dd, 2H), 4.25 (d, 1H), 4.12 (t, 1H), 4.03 (br, 1H), 3.14 (dd, 2H), 1.60-1.20 (m, 32H), 0.88 (t, 3H).

1.2.8. Synthesis of Isocyanate-terminated PEG (PEG-NCO)

Poly (ethylene glycol) methyl ether (2 g, 1 mmol), previously azeotropically dried from toluene under high vacuum, was dissolved in dry toluene (20 mL) under inert atmosphere. Hexamethylene diisocyanate (1.6 ml, 10 mmol) and a trace amount of DBTDL were added into the solution. The mixture was heated at 40 °C under stirring and nitrogen atmosphere for 2 h. The polymer was precipitated in cold hexanes (200 mL) twice from a concentrated toluene solution, taking extreme care to keep the polymer under inert atmosphere as much as possible.

The resulting PEG-NCO was dried under high vacuum to yield a solid white material for characterization. ^{1}H NMR (400 MHz, $CDCl_3$) δ 4.83 (br, 1H), 4.21 (t, *J* = 4.8 Hz, 2H), 3.83 – 3.42 (backbone), 3.37 (s, 3H), 3.30 (t, *J* = 6.6 Hz, 2H), 3.16 (q, *J* = 6.7 Hz, 2H), 1.67 – 1.20 (m, 8H). SEC (THF) $M_{n,\,2k}$ = 4,730 g/mol, $Đ_{2k}$ = 1.10; $M_{n,\,10k}$ = 10,600 g/mol, $Đ_{10k}$ = 1.008.

1.2.9. Synthesis of Hindered-urea Terminated PEG (PEG-HU)

Dried PEG-NCO (1.75 g, 0.8 mmol) and *N-tert*-butylmethylamine (0.945 mL, 8 mmol) were dissolved in dry toluene (35 mL) under inert atmosphere. The mixture was stirred at room temperature for 2 h. The product was then precipitated 4 times in cold hexane (350 mL) from a concentrated toluene solution and dried to yield PEG-HU as a solid white material. ^{1}H NMR (400 MHz, $CDCl_3$) δ 4.86 (br, 1H), 4.28 (br, 1H), 4.20 (t, *J* = 4.7 Hz, 2H), 3.83 – 3.42 (backbone), 3.37 (s, 3H), 3.16 (m, 4H), 2.81 (s, 3H), 1.48 (m, 4H), 1.38 (s, 9H), 1.33 (m, 4H). SEC (THF) $M_{n,\,2k}$ = 3,130 g/mol, $Đ_{2k}$ = 1.10, $M_{n,\,10k}$ = 13,000 g/mol, $Đ_{10k}$ = 1.07.

1.2.10. Synthesis of Disperse Orange 3-terminated PEG (PEG-DO3)

PEG-HU (1 g, 0.5 mmol) was dissolved in dry DMSO along with DO3 (1.21 g, 5 mmol). The solution was heated to 120°C under vacuum (200 mbar) for 2 hours to remove the urea blocking group without evaporating the solvent. The DMSO was removed via liquid-liquid extraction with water and chloroform, where the DMSO went into the aqueous layer and the product remained in the organic layer. After concentrating, the organic layer was precipitated in diethyl ether 3 times before drying and characterizing the resulting PEG-DO3. ^{1}H NMR (400 MHz, $CDCl_3$) δ 8.41 – 7.55 (ar, 8H), 5.70 (br, 1H), 5.10 (br, 1H), 4.20 (t, *J* = 4.7 Hz, 2H), 3.83 – 3.42 (backbone), 3.37 (s, 3H), 3.22 (m, 4H), 1.48 (m, 4H), 1.33 (m, 4H).

1.2.11. Synthesis of Polycaprolactone (PCL)

Benzyl alcohol (0.24 mL, 23.1 mmol), 1,5,7-triazabicyclo[4,4,0]dec-5-ene (6.4 mg, 0.05 mmol, 0.1 mol%), and ε-caprolactone (5 mL, 462.4 mmol) were mixed under inert atmosphere. The mixture was heated at 60 °C for 4 hours, then quenched with benzyl alcohol (2.5 mL). The polymer was precipitated 5 times in cold diethyl ether (200 mL) from concentrated solution of

THF and dried to yield PCL as a white solid material. ^{1}H NMR (400 MHz, $CDCl_3$) δ 7.35 (ar, 5H), 4.05 (m, 2H), 2.30 (m, 2H), 1.64 (m, 4H), 1.38 (m, 2H). SEC (THF) M_n = 9,070 g/mol, Đ = 1.23.

1.2.12. Synthesis of PCL end-functionalize isocyanate (PCL-NCO)

PCL (2.051 g, 1.26 mmol), previously azeotropically dried from toluene under high vacuum, was dissolved in dry THF (100 mL) under inert conditions. Hexamethylene diisocyanate (3 mL, 25 mmol) and a tiny amount of DBTDL were added into the solution. The mixture was heated at 40 °C under stirring and nitrogen atmosphere for 2 h. The polymer was precipitated 4 times in cold diethyl ether (100 mL) from a concentrated THF solution and dried to yield PCL-NCO as a white solid material. ^{1}H NMR (400 MHz, $CDCl_3$) δ 7.35 (ar, 5H), 4.68 (br, 1H), 4.06 (m, backbone), 3.30 (m, 2H), 3.16 (m, 2H), 2.30 (m, backbone), 1.64 (m, backbone), 1.51 (m, 4H), 1.38 (m, backbone), 1.28 (m, 4H). SEC (THF) M_n = 14,300 g/mol, Đ = 1.43.

1.2.13. Synthesis of PCL end-functionalize hindered urea (PCL-HU)

Dried PCL-NCO (1.72 g) and *N-tert*-butylmethylamine (2 mL, 16.68 mmol) were dissolved in dry THF (60 mL) under inert atmosphere. The mixture was stirred at room temperature for 2 h. The product was then precipitated 4 times in cold ether (100 mL) from a concentrated THF solution and dried to yield PCL-HU as a solid white material. ^{1}H NMR (400 MHz, $CDCl_3$) δ 7.35 (ar, 5H), 4.74 (br, 1H), 4.29 (br, 1H), 4.06 (m, backbone), 3.16 (m, 4H), 2.81 (s, 3H), 2.30 (m, backbone), 1.64 (m, backbone), 1.50 (m, 4H), 1.38 (m, backbone + 9H), 1.25 (m, 4H). SEC (THF) M_n = 11,100 g/mol, Đ = 1.34.

1.2.14. Synthesis of Poly(Butyl Acrylate) (PBA-Br)

PBA-Br was synthesized via Cu(0)-mediated living radical polymerization, following a published procedure.[52] In brief, butyl acrylate was filtered through basic alumina to remove any inhibitor, then the initiator (EBiB) (1 eq.), monomer (targeting 10,000 g/mol at 50% conversion), $CuBr_2$ (0.05 eq.), and DMF (targeting 75 vol.% relative to all other reactants) were all added to a round-bottom flask. The flask was sparged with inert gas for 15 minutes before adding the Me6TREN ligand (0.12 eq.). A stir bar was wrapped in 10 cm of copper wire and cleaned with concentrated HCl, then rinsed with acetone and DMF before dropping it into the flask to begin the reaction. NMR aliquots were taken every 30 minutes to track conversion and the reaction was quenched by opening it to air and removing the stir bar once it reached 50% conversion. The polymer was purified by rotary evaporation of any remaining monomer, redissolving in DCM, running it through a neutral alumina plug to remove the copper and ligand, then drying on high vacuum overnight before characterizing. The pure polymer was characterized with ^{1}H NMR and SEC to confirm the product. ^{1}H NMR (400 MHz, $CDCl_3$) δ 4.03 (m, 2H), 2.28 (m, 1H), 1.90 (m, 1H), 1.60 (m, 3H), 1.37 (m, 2H), 0.93 (m, 3H). SEC (THF) M_n = 13,000 g/mol, Đ = 1.21.

1.2.15. Preparation of Thio-HU for End Group Functionalization

Thio-HU was synthesized in a two-step process before being added to the polymer chain end. First, an allyl-hindered urea was synthesized by mixing allyl isocyanate (1 eq.) with *N-tert*-butylmethylamine (1.1 eq.) at 1M concentration in DCM. The resulting allyl-HU was purified with high vacuum to remove all solvent and remaining reactants, resulting in a white solid, before characterizing with ^{1}H NMR and high-resolution mass spectrometry. ^{1}H NMR (400 MHz, $CDCl_3$) δ 5.87 (ddt, *J* = 17.2, 10.2, 5.6 Hz, 1H), 5.14 (dq, *J* = 17.2, 1.7 Hz, 1H), 5.06 (dq, *J* = 10.2, 1.5 Hz, 1H), 4.33 (br, 1H), 3.80 (tt, *J* = 5.6, 1.6 Hz, 2H), 2.82 (s, 3H), 1.37 (s, 9H). ^{13}C NMR (101 MHz, $CDCl_3$) δ 159.09 (C = O), 136.13 (C = **C** – C), 115.40 (**C** = C), 55.71 (C), 43.31 (C = C – **C**), 31.84 (CH_3), 29.05 ($3CH_3$). HRMS (ESI) *m*/*z*: $[M + H]^+$ calcd for $C_9H_{18}N_2O$, 171.1453; found, 171.1497.

A thiol group was added to the allyl-HU by dissolving 1 eq. of allyl-HU in 15 eq. of 1,6-hexanedithiol along with 0.5 eq. DMPA photoinitiator. Once dissolved, the solution was placed on a low-power UV source (bug zapper) for 30 minutes. The resulting thio-HU molecule was purified by loading the crude mixture onto a silica column with 9:1 hexanes:ethyl acetate. This 9:1 mixture pushed the excess dithiol and initiator fragments through, while retaining the product in the column. The product was then flushed from the column using pure ethyl acetate. Thio-HU was then dried as a yellow oil before characterization with ^{1}H NMR and high resolution mass spectrometry. ^{1}H NMR (400 MHz, $CDCl_3$) δ 4.51 (br, 1H), 3.27 (td, J = 6.7, 5.6 Hz, 2H), 2.80 (s, 3H), 2.57 – 2.44 (m, 6H), 1.78 (qi, J = 6.9 Hz, 2H), 1.65 – 1.50 (m, 4H), 1.37 (m, 13H), 1.31 (t, J = 7.8 Hz, 1H). ^{13}C NMR (101 MHz, $CDCl_3$) δ 159.36 (C = O), 55.62 (C), 40.08 (C – N), 33.94 (CH_2), 32.16 (S – C), 31.88 (CH_3), 30.01 (CH_2), 29.96 (CH_2), 29.51 (CH_2), 29.08 ($3CH_3$), 28.39 (CH_2), 28.02 (CH_2), 24.64 (CH_2). HRMS (ESI) m/z: $[M + H]^+$ calcd for $C_{15}H_{32}N_2OS_2$, 321.1990; found, 321.2041.

1.2.16. Synthesis of Hindered Urea-Terminated PBA (PBA-HU)

Thio-HU was added to PBA-Br chain ends via nucleophilic substitution. The bromine-terminated polymer (1 eq.) was dissolved in acetone at 500 mg/mL along with TEA (10 eq.). The solution was then purged with inert gas for 5 minutes before adding thio-HU (2 eq.). The reaction was allowed to proceed for 24 hours before another 2 eq. of thio-HU were added under inert atmosphere. This process was repeated until 5 total additions were made, totaling 10 eq. of thio-HU. The resulting HU-terminated PBA-HU was purified by running the crude solution through a silica plug with 65:35 hexanes:ethyl acetate, where the PBA-HU eluted first, followed by the other reagents. The products were then dried before characterization with ^{1}H NMR and SEC. ^{1}H NMR (400 MHz, $CDCl_3$) δ 4.51 (br, 1H), 4.03 (m, backbone), 3.29 (m, 2H), 2.81 (s, 3H), 2.52 (m, 6H), 2.27 (m, backbone), 1.90 (m, backbone), 1.80 (m, 4H), 1.60 (m, backbone), 1.39 (s, 9H), 1.37 (m, backbone), 0.93 (m, backbone). SEC (THF) M_n = 11,900 g/mol, Đ = 1.04.

1.2.17. Functionalization of *c*-CNC-*g*-*Polymer* in Melt

The *c*-CNC-COOH (30 to 200 mg) were dispersed in 25 mL of deionized water by ultrasonication for 15 min, then solvent exchanged into acetone (see below). Relative to the CNC mass, hindered-urea-terminated polymer of the desired molar ratio was added to the CNC suspension and placed in a sonic bath until completely dissolved. The solvent was removed under high vacuum overnight to yield a dried powder. Once dry, the mixture was placed in an oil bath at 130°C and 120 mbar vacuum was applied to pull off the released volatile amine. After 2 hours, heat was removed and a mixture of water/acetone in a 1:1 ratio (50 mL) was added to the PEG grafting reactions, or THF for PCL and PBA reactions. The mixture was centrifuged and resuspended in the same solvent 10 times to remove non-attached polymer. The resulting *c*-CNC-*g*-*Polymer* were suspended in water and freeze-dried to obtain a fluffy powder.

1.2.18. Measuring Non-Grafted Polymer Chains

A UV-Vis calibration curve was created for PEG-DO3 in 1:1 water/acetone mixture from 100 mM to 10 nM. The functionalization of *c*-CNC-*g*-PEG was carried out as described before. After the grafting reaction was completed, a mixture of water/acetone in a 1:1 ratio (50 mL) containing 1 eq. of PEG-DO3 (relative to the PEG-HU added to the original reaction) was added to the medium. The mixture was centrifuged and resuspended in the same solvent couple, and the supernatants were analyzed with UV-Vis spectroscopy to track the removal of non-grafted polymer.

1.2.19. Solvent Exchange of CNCs

To disperse CNCs in non-aqueous solvents such as acetone, solvent exchange can be done to improve the quality of the suspension. In essence, 100 mg of CNCs are dispersed in 20 mL of DI water in a centrifuge tube using an ultrasonic bath before adding 20 mL of acetone. After mixing, the acetone/water suspension is centrifuged (10,000 g for 10 minutes) and the supernatant is poured off and replace by another 1:1 mixture of acetone:water. The precipitate is resuspended using a sonic bath and vortexer before centrifuging once again. The supernatant is then poured off and replace by pure acetone. Once the precipitate is resuspended, the CNCs form a more stable dispersion in acetone.

1.2.20. CNC + PCL and CNC + PBA FTIR Calibration Curves

To measure the polymer content of grafted CNCs, FTIR calibration curves were generated for PCL and PBA. In a small vial, 5-10 mg of *c*-CNC-COOH were mixed with the desired amount of polymer using a 20 mg/mL stock solution in MeOH to target samples with 5, 10, 15, 20, and

25 wt.% polymer. Minimal additional MeOH was added, and a spatula was used to ensure thorough mixing. The vials were immediately placed under high vacuum to remove the methanol and ensure a uniform distribution of polymer within the CNCs. Once dry, the samples were analyzed using FTIR and a calibration curve was developed based the representative carbonyl peak of each polymer (1724 cm^{-1} for PCL, and 1730 cm^{-1} for PBA).

1.2.21. Preparation of PLA + CNC composites

A 10 wt.% PLA stock solution was prepared by dissolving 30 g of PLA in 270 g of $CHCl_3$. Films with 5 wt.% *c*-CNC-*g*-PEG_{2k} and *c*-CNC-*g*-PEG_{10k} were prepared. The desired CNCs (e.g. 50 mg) were directly suspended in 20 ml of $CHCl_3$ using a sonic bath and vigorous shaking. The 10 wt.% PLA stock solution (10.0 g) was then added to the CNC suspension and thoroughly mixed. The resulting solution was allowed to mix in a sonic bath for a few hours and then cast into a Teflon petri dish to dry overnight. After removing the films from the petri dish, they were further dried in a vacuum oven at 60 °C for 48h before melt-pressing at 120 °C to obtain films of uniform thickness.

1.2.22. Tensile testing of composites

Tensile testing of composite materials was conducted following the ASTM D1708 standard. The video extensometer was used to monitor the elongation before yielding, while the crosshead distance was used to monitor the elongation after yielding, providing more accurate elongation measurements in the elastic regime and accounting for uneven plastic deformation after yielding. All samples were tested in triplicate and the average tensile strength and elongation at break were extracted for each sample.

1.3. Instrumentation

Atomic Force Microscopy (AFM) was done with a Cypher ES Environmental equipped with FS-1500 probes (Asylum Research) to determine the dimensions of CNCs. Crystals were dispersed in water by ultrasonication (10 min, 25% power, 3 s on/off cycle) at a concentration of 0.01% (w/w). A mica surface was mechanically exfoliated, treated with 50 μL poly(L-lysine), gently rinsed with DI water, then 50 μL of the freshly prepared CNC dispersion was drop-cast onto the surface. The dispersions were gently rinsed with DI water after 3 minutes and substrates were air-dried overnight prior to imaging. The images were recorded using tapping mode and the data was analyzed with Gwyddion software (Czech Metrology Institute).

Conductometric titrations of carboxylate and sulfate functional groups on the surface of the CNCs were performed using an Accumet XLbenchtop pH/conductivity meter on aqueous solutions. In brief, 30 mg of the desired CNCs were dispersed in 80 mL of DI water using probe sonication. For *c*-CNC-COOH the solution was acidified to a pH of 2-3 using concentrated HCl, then 0.01 M NaOH was titrated in using a syringe pump. For *c*-CNC-OSO_3, 0.01 M NaOH was directly titrated without acidification. Data was recorded at regular intervals and plotted as Conductivity vs. Volume added to determine the functional group content of the nanoparticles.

Fourier transform infrared (FTIR) spectroscopy of solid samples was carried out using a Shimadzu IRTracer-100 Fourier transform infrared spectrometer in the attenuated total reflection (ATR) geometry with a monolithic diamond ATR crystal. The sample temperature was controlled under a vacuum using the PIKE GladiATR accessory. Data was collected in the range of 4000–400 cm^{-1}, averaging over 45 scans, and treated with Shimadzu LabSolutions IR software.

High resolution mass spectrometry (HRMS) was performed on an Agilent 6224 ToF-MS using electrospray ionization (ESI).

Nuclear magnetic resonance (NMR) was carried out at ambient temperature on a Bruker Avance II+ 400 spectrometer at frequencies 400 MHz for ^{1}H nuclei and 101 MHz for ^{13}C nuclei. Spectra were calibrated to the residual solvent peak of $CDCl_3$ (7.26 ppm ^{1}H NMR, 77.16 ppm for ^{13}C NMR) and processed with MestReNova software. All chemical shifts, δ, are reported in parts per million (ppm) with coupling constant in Hz (multiplicity: s = singlet, d = doublet, dd = double doublet, td = triple doublet, t = triplet, dt = double triplet, tt = triple triplet, ddt =

double double triplet, q = quadruplet, dq = double quadruplet, qi = quintuplet, m = multiplet, br = broad signal, ar = aromatic signal).

Size exclusion chromatography (SEC) of the polymers was performed on a Shimadzu Prominence High Performance Liquid Chromatography system using an eluent mobile phase of THF at a flow rate of 1 mL/min. Separation was achieved using two PLgel mixed-D columns (Agilent) maintained at ambient temperature with pore sizes suitable for materials with effective molecular weights from ~200 to 400,000 g/mol. The differential refractive index signal was collected using a Wyatt Optilab T-rEX differential refractometer (λ = 658 nm), and on-line multi-angle light scattering (MALS) measurement was performed using a Wyatt Dawn Heleos II light scattering detector. Data analysis was carried out using Wyatt Astra VII software. Weight-averaged molecular weights (M_w) were determined by MALS, and number-average molecular weights (M_n) were determined in comparison to narrow dispersity polystyrene calibration standards (from 1,800 to 400,000 g mol^{-1}).

Thermogravimetric analysis (TGA) was performed using a TA Instruments Discovery thermogravimetric analyzer. Samples (~5mg) were loaded in Pt crucibles and heated under a N_2 atmosphere. High resolution dynamic procedure with default settings (sensitivity=1, ramp=10 to 700 °C, resolution=5) were applied. Data was processed in TA Instruments Trios software.

Wide-angle X-ray scattering (WAXS) patterns were recorded using a SAXSLAB GANESHA 300XL system with Cu Kα source (λ= 0.154 nm) at a voltage of 40 kV and 40 mA power. Powder samples were tightly packed inside plastic washers and were held in place between two pieces of Kapton tape. The data were collected in the 2-theta angle range of 1-32° for 20 minutes. The crystallinity index was calculated using MATLAB R2018a by modelling the (1,-1,0), (1,1,0), (1,0,2), and (2,0,0) cellulose-1β peaks and the residual amorphous component to Gaussian distribution functions as described previously.[53,54]

Probe Ultrasonication was carried out on a Branson SFX 550 instrument equipped with a 13 mm probe. Sonication was conducted at 20% amplitude with 5 seconds on and 5 seconds off per cycle while the sample vial was submerged in ice water to prevent significant heating.

Ultraviolet-Visible Light (UV-Vis) Spectroscopy was conducted on a Shimadzu UV-3600 Plus UV-Vis-NIR spectrophotometer from 350-800 nm wavelengths. Samples were run at 1 nm resolution in quartz cuvettes.

Melt Pressing was done on a Carver AccuStamp Model 3693 melt press at 120 °C at 2 tons of pressure for 3 minutes.

Tensile testing was conducted with a Zwick-Roell zwickiLine Z0.5 instrument. Dogbones in accordance with ASTM D1708 were measured up to the yield point with a VideoXtens extensometer, then by crosshead tracking after yielding.

Dynamic mechanical analysis (DMA) was performed on a TA Instruments RSA-G2 DMA on films of each sample (~ 3 mm x 1 mm x 20 mm). Temperature ramps were run from 25 to 100 °C at 3 °C per min at a frequency of 1 Hz.

2. Supporting Figures

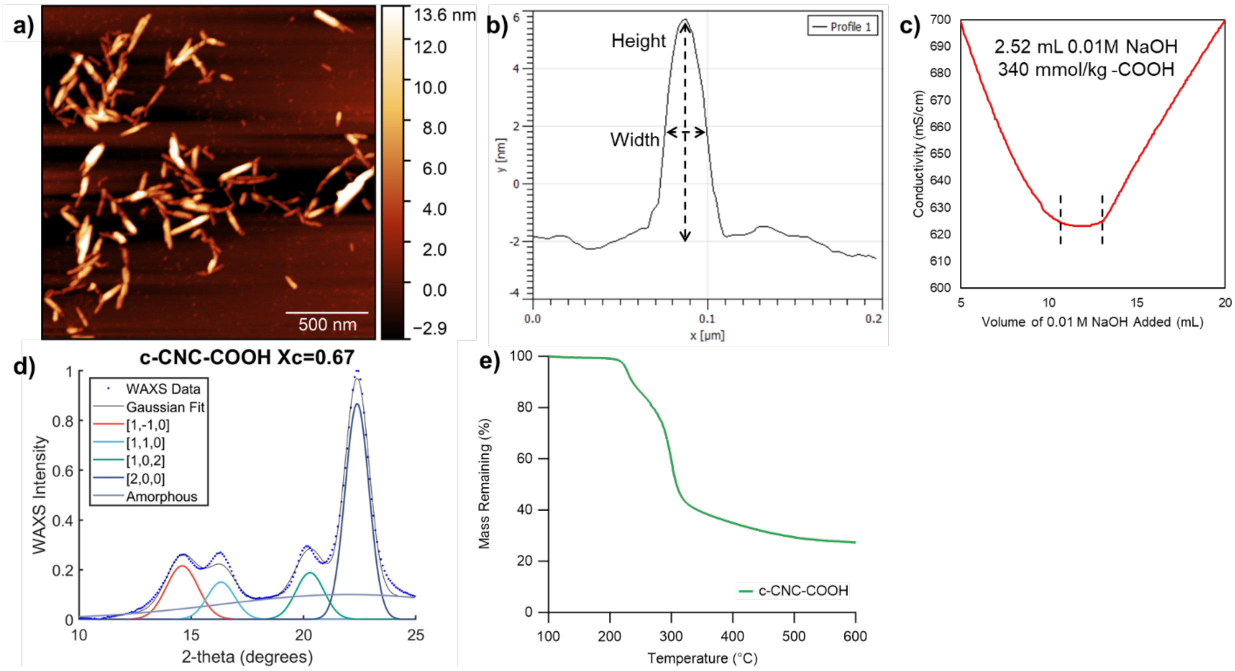

Figure S1. a) AFM height image of *c*-CNC-COOH, **b)** a height profile extracted from the AFM image showing how height and width of the nanoparticles are measured, **c)** a representative conductivity titration curve of *c*-CNC-COOH showing the weak acid plateau corresponding to -COOH neutralization, **d)** WAXS of *c*-CNC-COOH showing the crystallinity index, and **e)** the TGA degradation trace of the *c*-CNC-COOH.

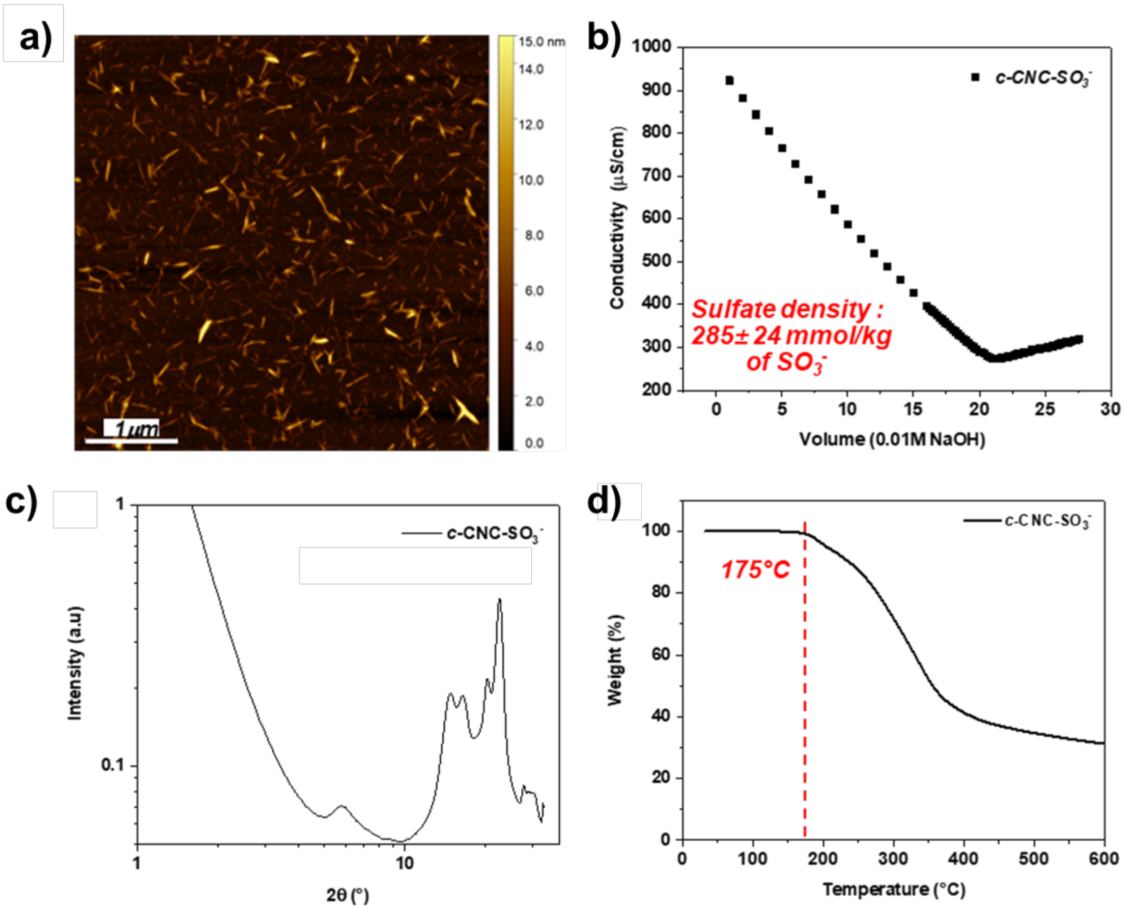

Figure S2. a) AFM height image of *c*-CNC-OSO3, **b)** a representative conductivity titration curve of *c*-CNC-OSO3, **c)** WAXS of *c*-CNC-OSO3 showing the crystallinity index, and **d)** the TGA degradation trace of the *c*-CNC-OSO3.

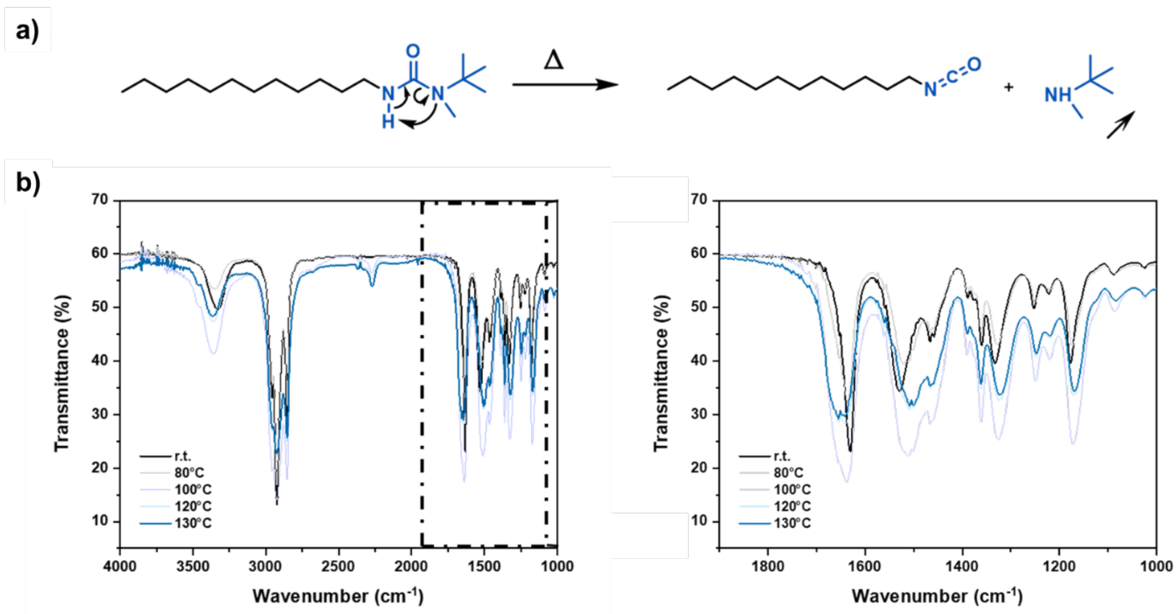

Figure S3. a) Scheme of hindered urea (dodecyl-HU) dissociation upon heating and **b)** FTIR spectra of the dodecyl-HU component at temperatures ranging from 80°C to 130°C, focusing on the signals at 1900-1000 cm^{-1}.

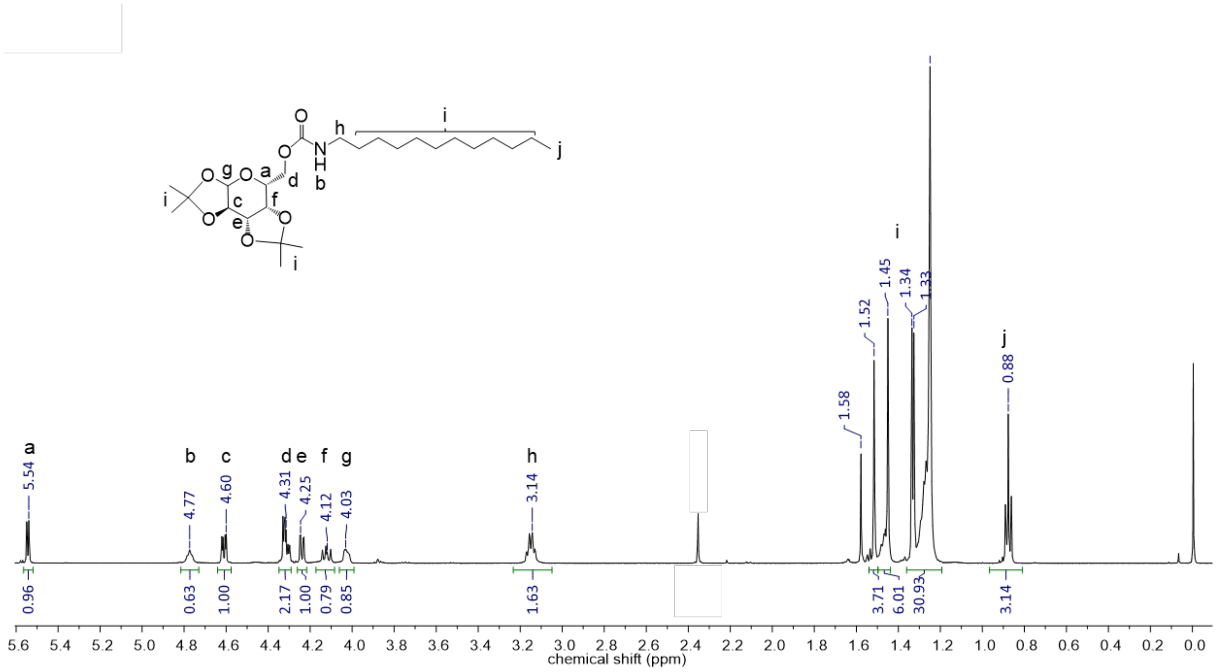

Figure S4. The [1]H NMR spectrum of the product resulting from the reaction of dodecyl-HU with PG with key peaks labeled.

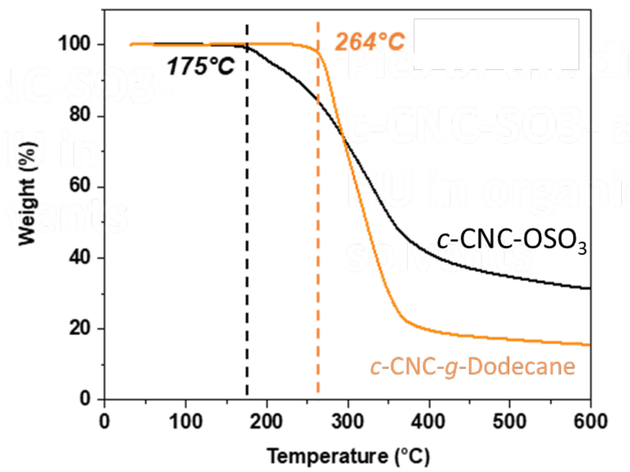

Figure S5. TGA of *c*-CNC-OSO_3 and *c*-CNC-*g*-dodecane showing increased thermal stability in the grafted CNCs.

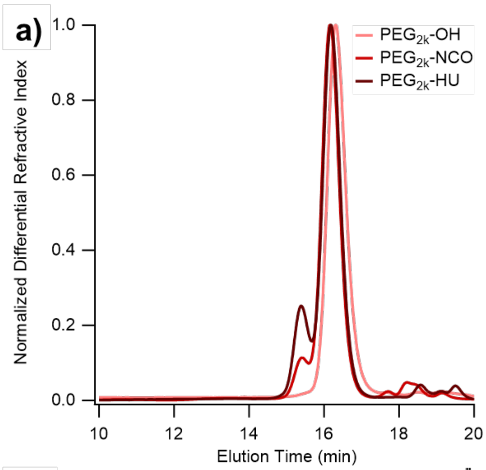

Sample	M_n (g/mol)	Dispersity Index(Đ)
PEG_{2k}-OH	1,850	1.27
PEG_{2k}-NCO	4,730	1.10
PEG_{2k}-HU	3,130	1.10

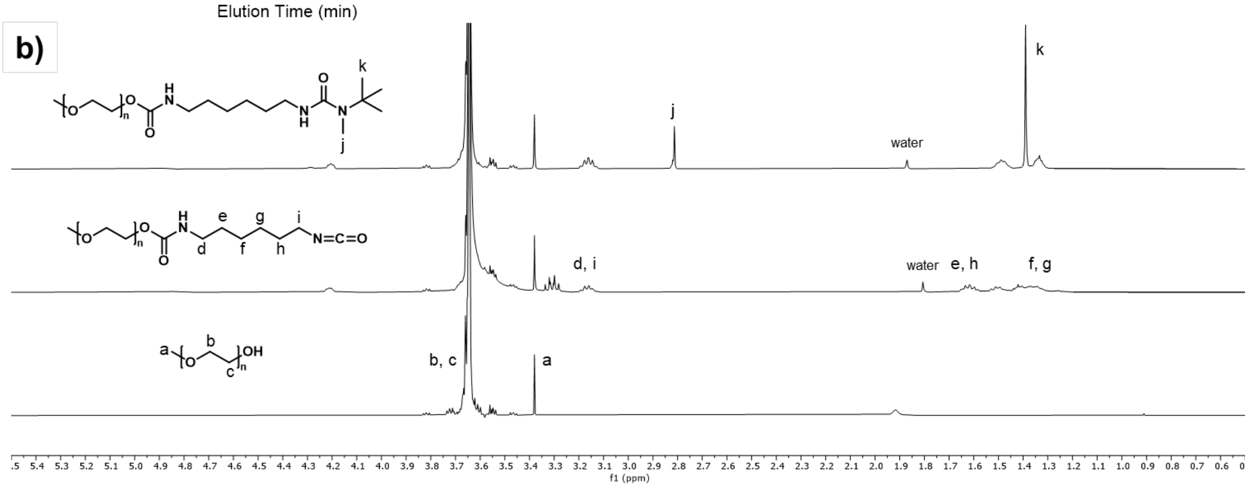

Figure S6. a) SEC traces and corresponding molecular weight and dispersity for PEG_{2k}-OH, PEG_{2k}-NCO, and PEG_{2k}-HU, and **b)** ^{1}H NMR spectra of PEG_{2k}-OH, PEG_{2k}-NCO, and PEG_{2k}-HU with key peaks labeled.

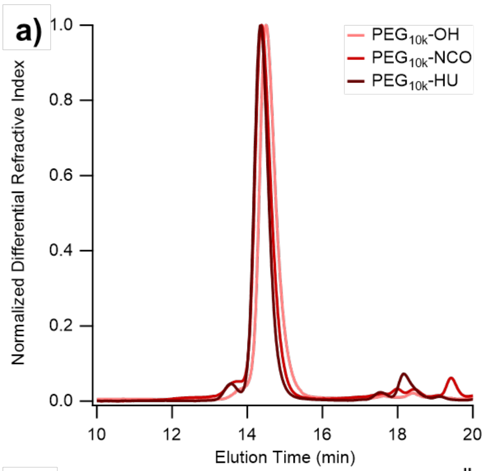

Sample	M_n (g/mol)	Dispersity Index(Đ)
PEG_{10k}-OH	10,100	1.002
PEG_{10k}-NCO	10,600	1.008
PEG_{10k}-HU	13,000	1.07

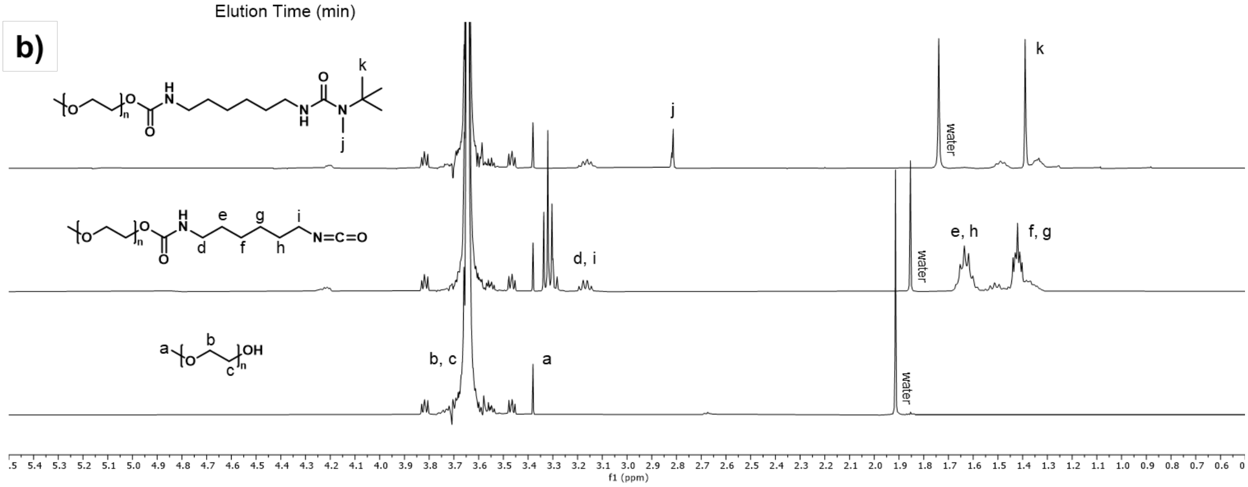

Figure S7. a) SEC traces and corresponding molecular weight and dispersity for PEG_{10k}-OH, PEG_{10k}-NCO, and PEG_{10k}-HU, and **b)** ^{1}H NMR spectra of PEG_{10k}-OH, PEG_{10k}-NCO, and PEG_{10k}-HU with key peaks labeled.

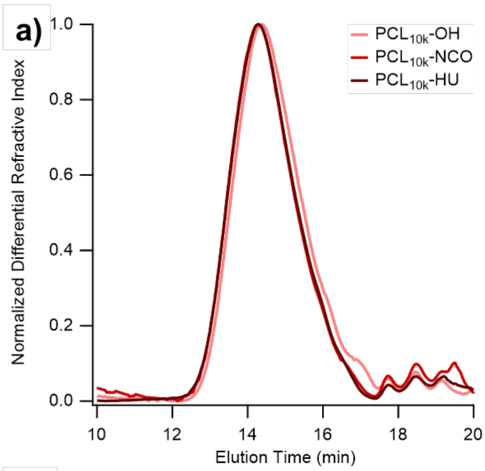

Sample	M_n (g/mol)	Dispersity Index(Đ)
PCL_{10k}-OH	9,070	1.23
PCL_{10k}-NCO	14,300	1.43
PCL_{10k}-HU	11,100	1.34

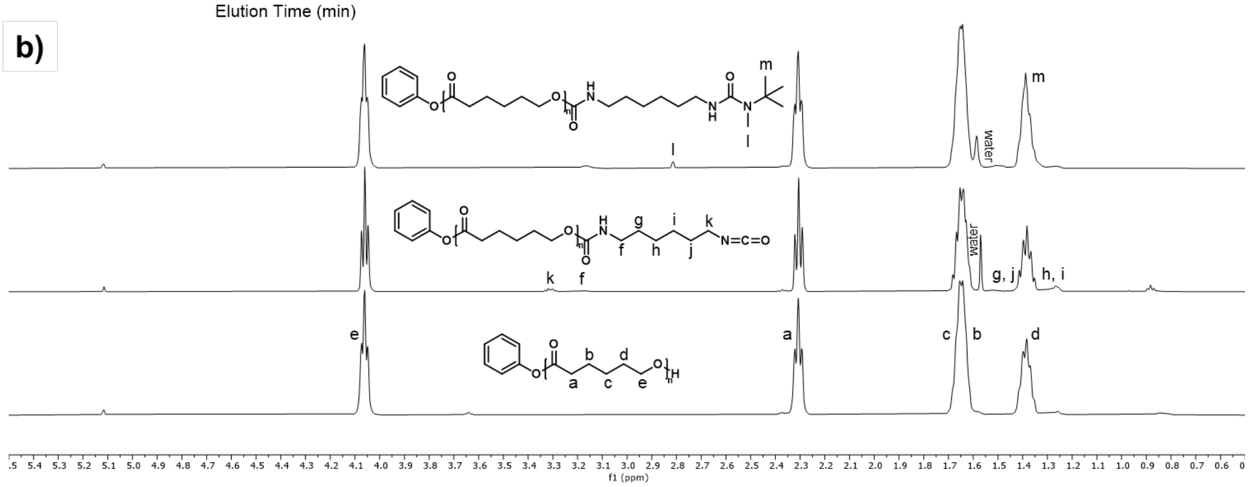

Figure S8. a) SEC traces and corresponding molecular weight and dispersity for PCL_{10k}-OH, PCL_{10k}-NCO, and PCL_{10k}-HU, and **b)** ^{1}H NMR spectra of PCL_{10k}-OH, PCL_{10k}-NCO, and PCL_{10k}-HU with key peaks labeled.

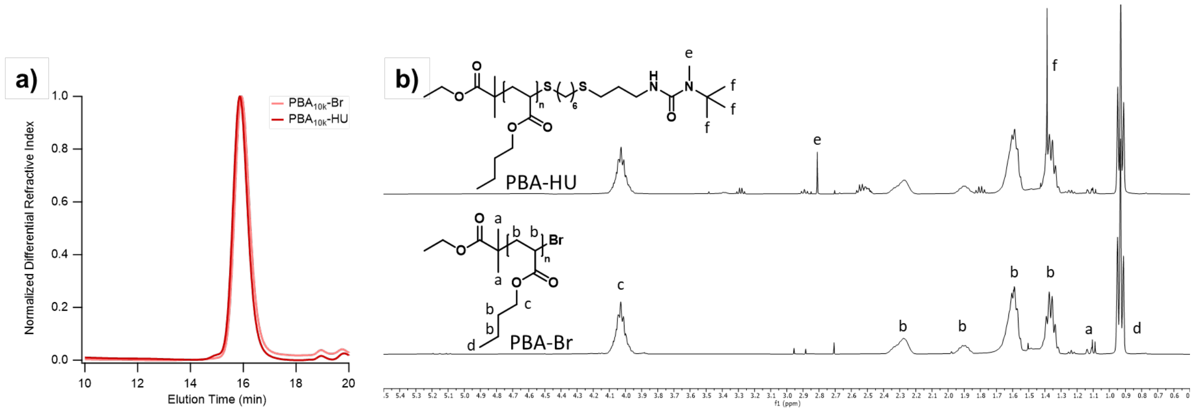

Figure S9. a) SEC traces for PBA_{10k}-Br and PBA_{10k}-HU and **b)** ^{1}H NMR spectra of PBA_{10k}-Br and PBA_{10k}-HU with key peaks labeled.

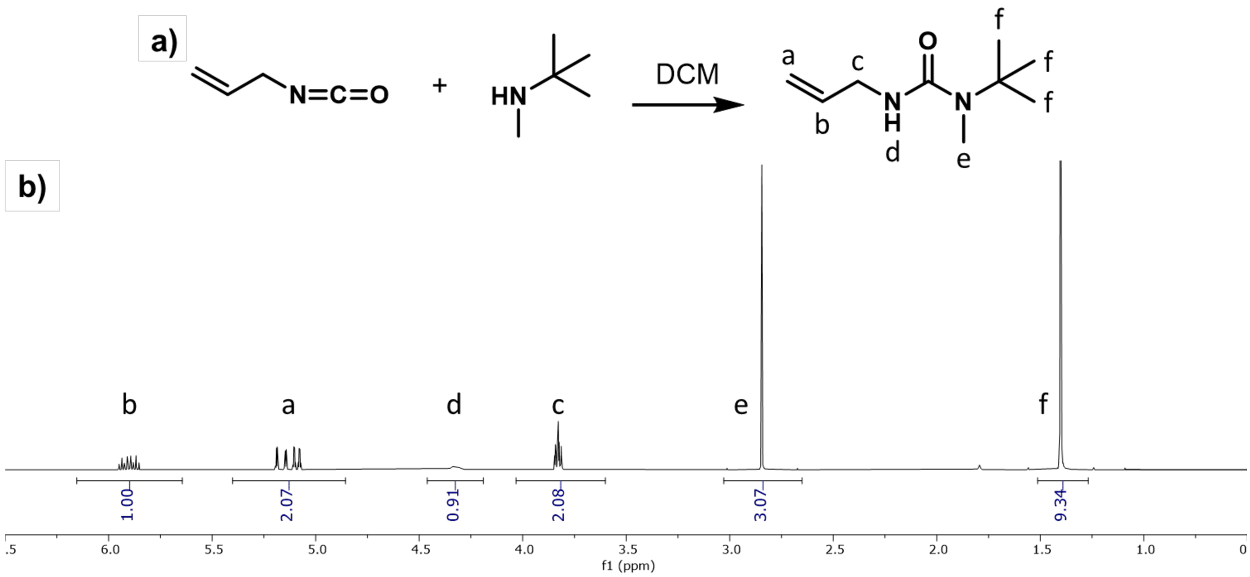

Figure S10. a) Schematic for the synthesis of allyl-HU from allyl isocyanate and *N-tert*-butylmethylamine and **b)** the resulting NMR spectrum.

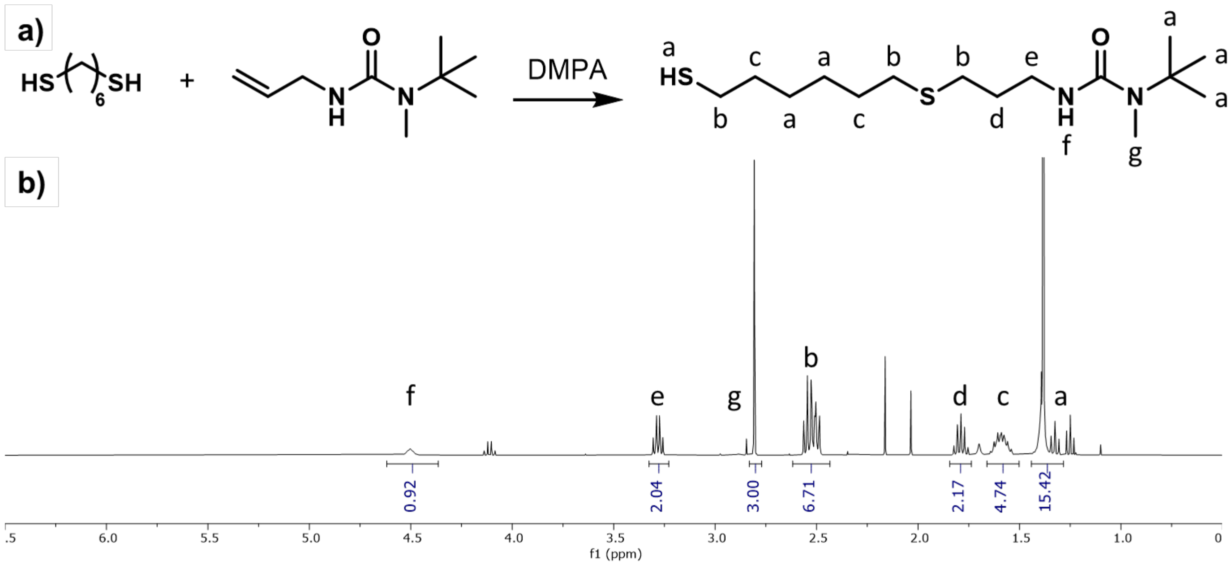

Figure S11. a) Schematic for the synthesis of thio-HU from allyl-HU and 1,6-hexanedithiol and **b)** the resulting NMR spectrum.

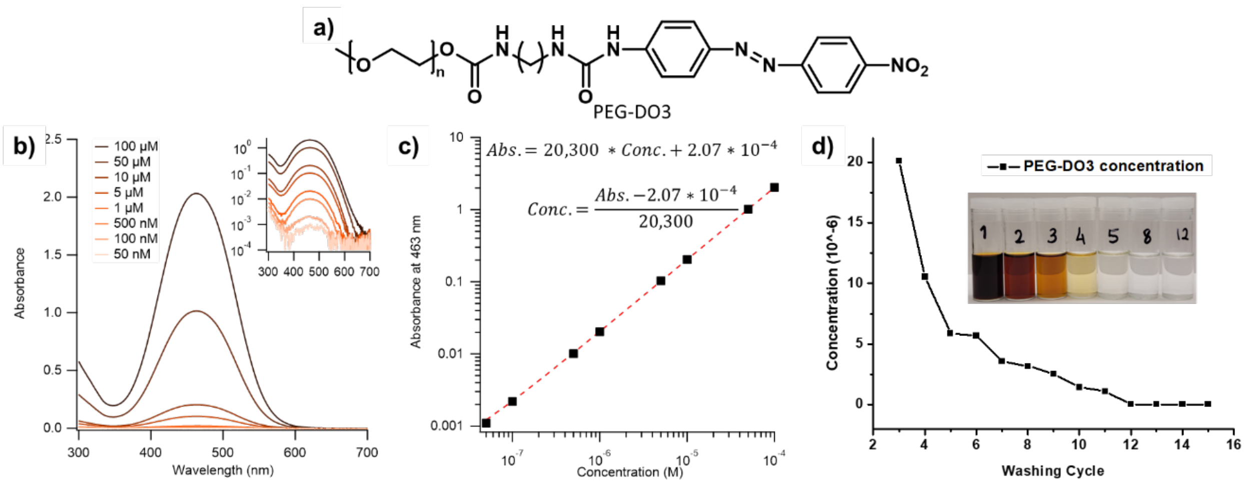

Figure S12. a) The chemical structure of PEG-DO3, **b)** UV-Vis traces of PEG-DO3 in 1:1 acetone:water with concentrations ranging from 50 nM to 100 µM, **c)** the resulting calibration curve generated from the maximum of the 463 nm absorbance peak, and **d)** the height of the 463 nm absorbance peak measured from supernatants generated during washing of *c*-CNC-PEG$_{2k}$ plotted against wash number, showing that all removable polymer is gone at wash 12.

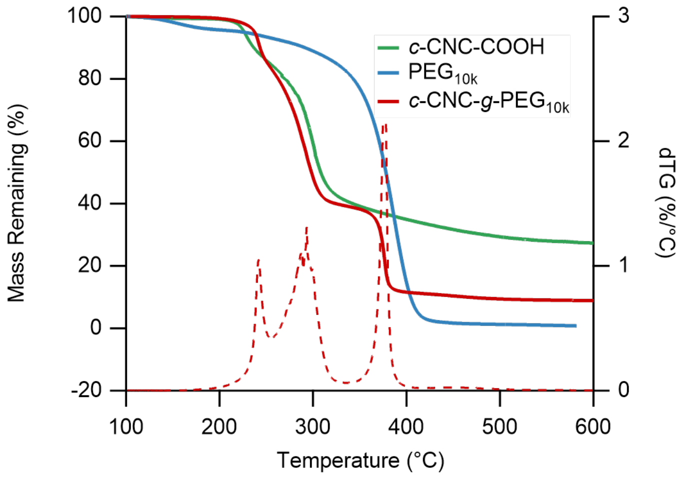

Figure S13. TGA traces of *c*-CNC-COOH, PEG$_{10k}$-Br, and *c*-CNC-*g*-PEG$_{10k}$ along with the dTG curve for *c*-CNC-*g*-PEG$_{10k}$.

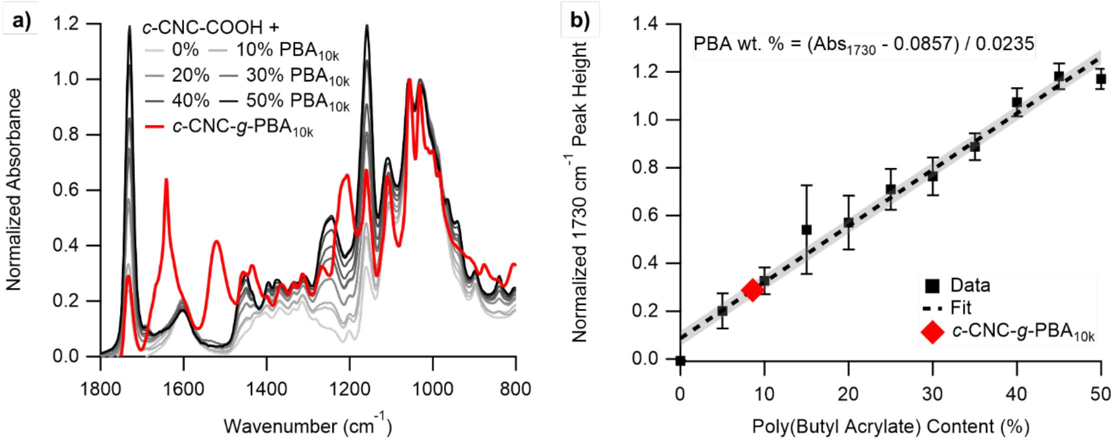

Figure S14. a) FTIR spectra for *c*-CNC-COOH mixed with various ratios of PBA_{10k}-Br and **b)** the resulting calibration curve to measure PBA content on grafted CNCs with the measured *c*-CNC-*g*-PBA_{10k} data placed on the curve.

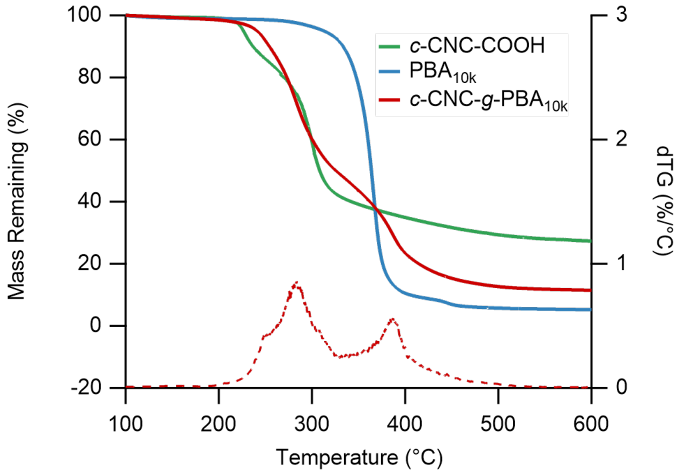

Figure S15. TGA traces of *c*-CNC-COOH, PBA_{10k}-Br, and *c*-CNC-*g*-PBA_{10k} along with the dTG curve for *c*-CNC-*g*-PBA_{10k}.

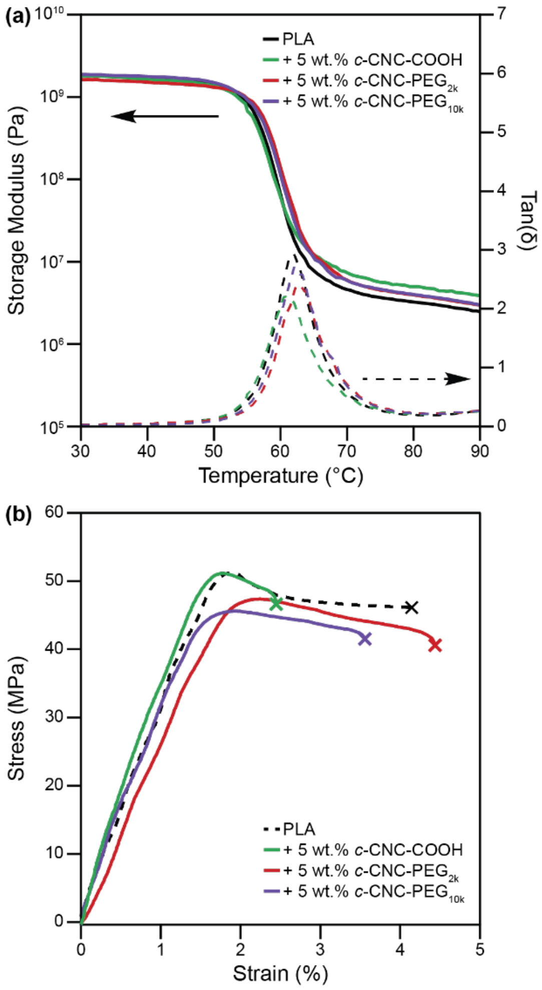

Figure S16: (a) Dynamic mechanical analysis data of PLA composites with 5 wt.% *c*-CNC-COOH, 5 wt.% *c*-CNC-*g*-PEG$_{2k}$, and 5 wt.% *c*-CNC-*g*-PEG$_{10k}$ compared to unmodified PLA, and (b) tensile testing data of neat PLA and composites with 5 wt.% *c*-CNC-COOH, 5 wt.% *c*-CNC-*g*-PEG$_{2k}$, and 5 wt.% *c*-CNC-*g*-PEG$_{10k}$.

3. References

[1] Fraschini, C., Chauve, G. & Bouchard, J. TEMPO-mediated surface oxidation of cellulose nanocrystals (CNCs). Cellulose 24, 2775–2790 (2017).

[2] Macke, N., Hemmingsen, C. M. & Rowan, S. J. The effect of polymer grafting on the mechanical properties of PEG-grafted cellulose nanocrystals in poly(lactic acid). J. Polym. Sci. 60, 3318–3330 (2022).

[3] Gille, A. & Hiersemann, M. (−)-Lytophilippine A: Synthesis of a C1− C18 Building Block. Org. Lett. 12, 5258–5261 (2010).

[4] Anastasaki, A. et al. Cu(0)-Mediated Living Radical Polymerization: A Versatile Tool for Materials Synthesis. Chem. Rev. 116, 835–877 (2016).

[5] French, A. D. Idealized powder diffraction patterns for cellulose polymorphs. Cellulose 21, 885–896 (2014).

[6] Park, S., Baker, J. O., Himmel, M. E., Parilla, P. A. & Johnson, D. K. Cellulose crystallinity index: measurement techniques and their impact on interpreting cellulase performance. Biotechnol. Biofuels 3, 1–10 (2010).